NASA CONTRACTOR REPORT

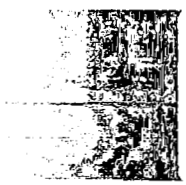

THE IGNITION OF SLOT-INJECTED GASEOUS HYDROGEN IN A SUPERSONIC AIR STREAM

by Joseph A. Schetz and Stanley Favin

Funded by NASA and Prepared under BUWEPS Contract No. NOw 62-0604-c *by*
JOHNS HOPKINS UNIVERSITY
Silver Spring, Md.
for

NATIONAL AERONAUTICS AND SPACE ADMINISTRATION • WASHINGTON, D. C. • JANUARY 1966

[redacted]

THE IGNITION OF SLOT-INJECTED GASEOUS HYDROGEN IN A SUPERSONIC AIR STREAM

By Joseph A. Schetz and Stanley Favin

Funded by NASA and Prepared under BUWEPS Contract No. NOw 62-0604-c by
JOHNS HOPKINS UNIVERSITY
Silver Spring, Md.

for

NATIONAL AERONAUTICS AND SPACE ADMINISTRATION

[redacted]

ABSTRACT

The effects of an initial air-side boundary layer on the ignition of slot-injected gaseous hydrogen by a hot supersonic air stream is treated analytically. The main parameters are shown to be boundary layer size, boundary layer character - laminar or turbulent, and hydrogen temperature. Comparison with previous experiment is made and general corroboration of the theory is obtained. Finally, some parametric numerical examples are presented and discussed.

NOTATION

A, B, C	Constants
b, $b_{\frac{1}{2}}$, $b'_{\frac{1}{2}}$	Characteristic widths in eddy viscosity models
C_p, C_{p_i}	Specific heat
h	Static enthalpy
H	Stagnation enthalpy
K	Constant
t	Transformed normal coordinate
T	Static temperature
T_o	Stagnation temperature
T_r	Reference temperature
u	Axial velocity
v	Normal velocity
v^*	Transformed normal velocity
W	Molecular weight
x	Axial coordinate
y	Normal coordinate
Y_i	Species mass fraction
ρ	Density
ϵ	Eddy viscosity
κ	Constant
Δ	Transformed boundary layer thickness
Δ^*	Transformed displacement thickness
ξ	Transformed axial coordinate
τ	Time
φ	Equivalence ratio
γ	Ratio of specific heats
δ	Physical boundary layer thickness
Subscripts	
c	Conditions along the extension of the splitter plate
e	Free stream conditions
j	Jet conditions
i = 1,2	Air and hydrogen respectively
w	Wall conditions

THE IGNITION OF SLOT-INJECTED GASEOUS HYDROGEN IN A SUPERSONIC AIR STREAM

Joseph A. Schetz* and Stanley Favin**

Applied Physics Laboratory
Johns Hopkins University
Silver Spring, Md.

INTRODUCTION

The recent interest in supersonic combustion phenomena[1,2,3] has created a need for the consideration of the always difficult question of ignition of gaseous fuels at now supersonic speeds. In general, we shall be interested in the ignition processes of mixing gas streams as, at least in most cases, the fuel is injected into the air stream at or near the entrance to the combustion region. The interesting but different case of the ignition of pre-mixed gases has been treated in the past rather extensively.[4,5]

The present writer has considered the general problem for a tangential wall slot injector configuration (see Fig. 1) in turbulent flow from a mainly experimental viewpoint with heated hydrogen as the fuel.[6] The principal result of this work, as far as the ignition question is concerned, was that experimental go, no-go ignition data could be correlated on the basis of the maximum static temperature in the air stream. The hydrogen fuel temperature used did not vary strongly (between 675-900°K). In particular, it was found that under conditions where the maximum air temperature was greater than 1000°K, ignition occurred and where $T_{max} \geq 1050^{\circ}K$, ignition was very rapid. The maximum static temperature in the air stream was determined by considering the supersonic boundary layer on the outside of the splitter plate at the injection station (see Fig. 2). Assuming the applicability of a Crocco integral between the velocity and the total temperature,[7]

$$T_o = Au + B$$

$$= (T_{oe} - T_w) \frac{u}{u_e} + T_w \qquad (1)$$

since $T_o \equiv T + u^2/2C_p$, the static temperature becomes

$$T = (T_{oe} - T_w) \frac{u}{u_e} + T_w - \frac{u^2}{2\bar{c}_p} \qquad (2)$$

To look for a maximum, one would ordinarily insert some velocity profile, u(y), differentiate with respect to "y" and set this derivative equal to zero, etc. Note that the specification of a velocity profile requires a statement as

* Consultant, also Assoc. Prof. of Aerospace Engrg., Univ. of Md., College Park, Md.

** Associate Mathematician

to whether the flow is laminar or turbulent. However, since the velocity itself is monatonic in y for either case, we may look for any maximum by differentiating with respect to "u", i.e.

$$\frac{dT}{du} = \frac{(T_{oe} - T_w)}{u_e} - \left(\frac{u_e^2}{2c_p}\right)\left(\frac{2u}{u_e^2}\right) \tag{3}$$

Thus

$$\left(\frac{u}{u_e}\right)_{T=T_{max}} = (T_{oe} - T_w)\left(\frac{c_p}{u_e^2}\right) \tag{4}$$

and

$$T_{max} = (T_{oe} - T_w)^2 \frac{c_p}{u_e^2} + T_w - \frac{1}{2}(T_{oe} - T_w)^2 \frac{c_p}{u_e^2} \tag{5}$$

$$= T_w + \frac{1}{2}\frac{(T_{oe} - T_w)^2}{u_e^2/c_p}$$

but $u_e^2/c_p = 2\,(T_{oe} - T_e)$, so that

$$T_{max} = T_w + \frac{1}{4}\frac{(T_{oe} - T_w)^2}{(T_{oe} - T_e)} \tag{6}$$

It is clear that further considerations are in order if one wishes to predict the probability of ignition under conditions of widely varying fuel temperature. Moreover, it seems certain that the physical size of the air boundary layer relative to the injection slot height and thus the amount of air that may be at the elevated static temperatures relative to the fuel flow is important here. Also in the case where the free stream static temperature is above the ignition temperature, but the boundary layer is cooler as a result of strong upstream cooling along the wall prior to injection, the size of the air boundary layer describes the size of the cool "buffer layer" between the fuel and the hot air.

In addition to the physical size of the boundary layer, it is clear that the distribution of static temperature through the layer is important. Since a laminar and turbulent boundary layer possess markedly different distributions, both cases should be considered and compared. The vortex sheet produced downstream of the injection station by the velocity difference between the free stream and the injectant will most likely produce transition and a fully turbulent mixing region, but the state of the initial boundary

can still be important. All of this would seem to warrant a detailed analytical study of ignition processes in the neighborhood of a splitter plate, paying particular attention to the influences of a boundary layer on the air side. While it is true that a boundary layer exists on the fuel side, it is generally much smaller than the air boundary layer since the air traverses a long run on the inlet before reaching the injection station and the fuel usually comes directly from a plenum chamber near the slot. Furthermore, the Mach number of the fuel as injected is generally low, often subsonic, so that the effects of viscous dissipation are much smaller in this region.

This report is thus concerned with a study of the flow field, shown schematically in Fig. 3. The flow in the mixing region is taken as fully turbulent and the effects of the wall which bounds the fuel jet on the bottom are neglected as being unimportant in the initial mixing region where we wish to study ignition processes. The logical first step in the treatment of this problem is to develop the flow field for a non-reacting or frozen situation. This is accomplished here by an extension of the writer's previous turbulent free jet mixing analysis.[8] Essentially, the treatment is based on the assumption of unit turbulent Prandtl and Lewis numbers, a mass flow difference model for the eddy viscosity and a linearization of the boundary layer equations performed in a Howarth-Dorodritzin plane, as opposed to the older analysis which was done in the Von Mises plane. The initial boundary layer profile is approximated by a modified exponential in the form:

$$\frac{u}{u_e} = 1 - e^{-A(\frac{t}{\Delta})}$$

By a variation of the value of the parameter, A, this expression can be made to represent either a laminar or turbulent boundary layer to a good degree of accuracy. A profile with A = 2.50 is compared with an experimental laminar profile[7] in Fig. No. 4 and one with A = 10.0 is compared with an experimental turbulent profile[7] in Fig. No. 5. The initial enthalpy profiles are related to the assumed velocity profiles by another form of the Crocco integral, namely

$$H = (H_e - H_w)(1 - e^{-A(\frac{t}{\Delta})}) + H_w \quad , \quad t \geq o$$

$$= H_j = \text{constant} \quad , \quad t < o \qquad (8)$$

Once the flow field is determined, an isotherm and streamline pattern can be constructed. These patterns can be examined to see if any regions exist with both T > Tig and the fuel concentration above the lean ignition limit. If not, ignition is not possible. If these conditions are met in a region then, the streamline through this area can be followed downstream to see if sufficient time for ignition is available before passing into a colder or leaner region.

In general, this procedure could be accomplished with a chemical kinetic analysis of premixed gases (e.g., Ref. 5) modified to allow distributed sources and sinks of heat along the path so that the "frozen" temperature history along the streamline can be matched. At first glance, it may seem strange to employ a non-reacting mixing analysis to determine the streamline temperature history, but it has been shown that essentially no net temperature rise is achieved during the ignition delay period. All the energy goes into the shuffling of the concentration of the various molecular and atomic constitutents. Thus, the local temperature field is not affected by the chemical reactions during this period and can be determined from a non-reactive analysis provided that dissociation of the molecular species, which does change the density, does not significantly affect the mixing process. In all this, the effects of varying overall equivalence ratio along the streamline could likely be neglected since it is well known that ignition delay times are quite insensitive to equivalence ratio over wide ranges. However, this effect could also be included by allowing distributed mass sources and sinks so that the local overall equivalence ratio predicted by the "frozen" analysis could be reproduced. In the present work, a cruder but quite useful procedure is employed. Previously determined,[4,5] ignition delay correlations are used to estimate an ignition delay time which is then compared to the residence time of a fluid particle in the "hot spot" in order to assess the likelihood of ignition.

An analysis of a related, but simpler, problem has been presented by Marble and Adamson.[9] They treated a laminar case with no initial boundary layer and a simple one-step combustion reaction. In that instance, the flow field is similar and can be handled simply; there is no problem with respect to the selection of an eddy viscosity model and the simple chemistry does not predict an ignition temperature and cannot be modified to reasonably represent the hydrogen and air reaction.[4]

ANALYSIS

Conservation Laws

The mixing of a non-homogeneous flow system can be described by the general laws of conservation of mass, momentum, energy and individual species for a compressible fluid. The turbulent laws are taken here to be identical in form to the corresponding laminar flow equations when expressed in terms of mean flow quantities and turbulent "eddy transport coefficients". Taking the turbulent Prandtl and Lewis numbers as unity, the boundary layer form of these laws for constant static pressure may be written:

Mass continuity

$$\frac{\partial(\rho u)}{\partial x} + \frac{\partial(\rho v)}{\partial y} = 0 \qquad (9)$$

Momentum

$$\rho u \frac{\partial u}{\partial x} + \rho v \frac{\partial u}{\partial y} = \frac{\partial}{\partial y} \left(\rho \epsilon \frac{\partial u}{\partial y}\right) \tag{10}$$

Energy (stagnation enthalpy)

$$\rho u \frac{\partial H}{\partial x} + \rho v \frac{\partial H}{\partial y} = \frac{\partial}{\partial y} \left(\rho \epsilon \frac{\partial H}{\partial y}\right) \tag{11}$$

Species

$$\rho u \frac{\partial Y_i}{\partial x} + \rho v \frac{\partial Y_i}{\partial y} = \frac{\partial}{\partial y} \left(\rho \epsilon \frac{\partial Y_i}{\partial y}\right) \tag{12}$$

where ϵ = eddy transport coefficient, i = 1,2 denoting air and hydrogen respectively.

It is convenient to transform these equations into a constant density form by the introduction of a new normal coordinate defined as

$$t \equiv \int_o^y \frac{\rho}{\rho_e} \, dy \tag{13}$$

In the (x,t) plane, the conservation laws become

$$\frac{\partial u}{\partial x} + \frac{\partial v^*}{\partial t} = 0 \tag{14}$$

$$u \frac{\partial u}{\partial x} + v^* \frac{\partial u}{\partial t} = \frac{1}{\rho_e^2} \frac{\partial}{\partial t} \left[(\rho^2 \epsilon) \frac{\partial u}{\partial t} \right] \tag{15}$$

$$u \frac{\partial H}{\partial x} + v^* \frac{\partial H}{\partial t} = \frac{1}{\rho_e^2} \frac{\partial}{\partial t} \left[(\rho^2 \epsilon) \frac{\partial H}{\partial t} \right] \tag{16}$$

$$u \frac{\partial Y_i}{\partial x} + v^* \frac{\partial Y_i}{\partial t} = \frac{1}{\rho_e^2} \frac{\partial}{\partial t} \left[(\rho^2 \epsilon) \frac{\partial Y_i}{\partial t} \right] \tag{17}$$

Eddy Viscosity Model

At this stage, we must specify a model for the term $(\rho^2 \epsilon)$ containing the eddy viscosity. There has been a considerable effort expended towards

determining a suitable form for this quantity over the last few years. The present writer has employed a generalization of Prandtl's low speed flow expression

$$\epsilon = Kb_{\frac{1}{2}}(x)\left|u_{max} - u_{min}\right| = f_1(x) \tag{18}$$

where

$$u(x,b_{\frac{1}{2}}) = \frac{u_{max} + u_{min}}{2}$$

following Ferri[10] to

$$\rho^2\epsilon = Kb'_{\frac{1}{2}}(x)\ \rho_c(x)\left|(\rho u)_{max} - (\rho u)_{min}\right| = f_2(x) \tag{19}$$

where

$$\rho u\ (x,b'_{\frac{1}{2}}) = \frac{(\rho u)_{max} + (\rho u)_{min}}{2}$$

in the treatment of two-dimensional free jet mixing of hydrogen in air.[8] Recent experiments on this system have been independently performed by the Marquardt Corp.[11] Some comparison between the theory and experimental results is shown in Fig. 6 with the kind permission of Mr. M. L. Brown. Clearly good agreement has been achieved, and one is encouraged to believe that an expression of the form of Eq. (19) can be used with some confidence. In attempting to translate all this to the present problem, it is instructive to consider the classical treatment of the low speed equivalent without an initial boundary layer.[12] In that case, the mixing width, b, was taken proportional to the streamwise coordinate, x, so that

$$\epsilon(x) = K(cx)\left|u_{max} - u_{min}\right| \tag{20}$$

further

$$\sigma = \frac{1}{2}(Kc\lambda)^{-\frac{1}{2}} \simeq 15 \text{ where } \lambda \equiv \frac{u_{max} - u_{min}}{u_{max} + u_{min}}$$

Finally, then, we can write

$$\epsilon(x) = \frac{x}{60}(u_e + u_j) \tag{21}$$

Extending this to the compressible, variable density case as in going from Eq. (18) to Eq. (19) we get

$$\rho^2\epsilon = \frac{\rho_c(x)\ x}{60}(\rho_e u_e + \rho_j u_j) = f_3(x) \tag{22}$$

This expression gives a zero eddy viscosity at the end of the splitter plate which is unrealistic in any case and cannot be for the case of an initial turbulent boundary layer which is of interest here. Clauser[13] has shown that the "wake" region of an incompressible turbulent boundary layer can be considered to have a constant eddy viscosity expressed as

$$\epsilon = K \Delta^* \quad u_e \tag{23}$$

where $K = .016$. We can, therefore, modify Eq. (22) to include this behavior approximately as

$$\rho^2 \epsilon = \frac{\rho_c(x)\ [x + \Delta_o^*]}{60} (\rho_e u_e + \rho_j u_j) \tag{24}$$

Solution in the Transformed Plane

Returning now to the differential equations of motion, the question of their solution must be considered. In the absence of an initial boundary layer, the flow problem is "similar" and the solution is straightforward. With the boundary layer, the problem is "non-similar", and either numerical or approximate methods must be employed. The crude nature of our present understanding of turbulent flow processes hardly justifies the expense and complication of a direct numerical solution. Rather, it seems appropriate to pursue some approximate method. Here, the use of a linearized approximation following Oseen and Carrier (see Ref. 14) has been chosen. Accordingly, the convective derivative is approximated as

$$u \frac{\partial(\ )}{\partial x} + v^* \frac{\partial(\ )}{\partial t} \cong u_e \frac{\partial(\ )}{\partial x} \tag{25}$$

rendering the Momentum Equation, for example, into the form

$$u_e \frac{\partial u}{\partial x} = \frac{\rho^2 \epsilon}{\rho_e^{\,2}} \frac{\partial^2 u}{\partial t^2} \tag{26}$$

This can be further simplified by the introduction of a new streamwise coordinate, ξ, defined by

$$\frac{dx}{d\xi} = \frac{\rho_e^{\,2}\ u_e}{\rho^2 \epsilon} \tag{27}$$

Using Eq. (11)[+]

$$(x + \Delta_o^*)\, dx = \frac{60\ (\rho_e/\rho_e)}{\left(1 + \frac{\rho_j u_j}{\rho_e u_e}\right)} \quad d\xi \tag{28}$$

and since $\xi\ (x = 0) = 0$, this becomes

$$\frac{x^2}{2} + \Delta_o^* x = \frac{60}{\left(1 + \frac{\rho_j u_j}{\rho_e u_e}\right)} \int_o^{\xi} (\rho_e/\rho_c)\, d\xi' \tag{29}$$

The momentum equation now takes the final form

$$\frac{\partial u}{\partial \xi} = \frac{\partial^2 u}{\partial t^2} \tag{30}$$

which can be easily recognized as the classical heat equation whose solution has been extensively studied.[15]

The boundary conditions pertinent to the problem of interest here are

$$\begin{aligned} u(o,t) &= u_e\ (1 - e^{-A(\frac{t}{\Delta})}) \qquad t \geq 0 \\ &= u_j \qquad\qquad\qquad\qquad t < 0 \\ \lim_{t\to(+\infty)} u(\xi,t) &= u_e \\ \lim_{t\to(-\infty)} u(\xi,t) &= u_j \end{aligned} \tag{31}$$

The solution is most easily obtained by the use of Green's functions and can

---

[+] For the case of a laminar initial boundary layer, the Δ_o^* is dropped and Eq. (22) must be modified accordingly.

be written:

$$\frac{u(\xi,t)}{u_e} = \frac{1}{2}\left[1 + \text{erf}\left(\frac{t}{\sqrt{4\xi}}\right)\right] + \frac{\tilde{u}_j}{2}\,\text{erfc}\left(\frac{t}{\sqrt{4\xi}}\right)$$

$$-e^{\left(\frac{A^2\xi}{\Delta^2} - \frac{At}{\Delta}\right)}\left[1 + \text{erf}\left(\frac{t}{\sqrt{4\xi}} - \frac{A\sqrt{\xi}}{\Delta}\right)\right] \qquad (32)$$

The stagnation enthalpy and species concentration fields are subject to the boundary conditions

$$H(o,t) = H_e - (H_e - H_w)\, e^{-A\left(\frac{t}{\Delta}\right)} \quad , \; t \geq 0$$

$$= H_j = \text{constant} \quad , \quad t < 0$$

$$Y_1(o,t) = 1 \quad , \quad t \geq 0 \qquad Y_2(o,t) = 0 \quad , \quad t \geq 0$$

$$= 0 \quad , \quad t \leq 0 \qquad\qquad = 1 \quad , \quad t \leq 0$$

$$\lim_{t\to(+\infty)} H(\xi,t) = H_e \quad ; \quad \lim_{t\to(-\infty)} H(\xi,t) = H_j \qquad (33)$$

$$\lim_{t\to(+\infty)} Y_1(\xi,t) = 1 \quad ; \quad \lim_{t\to(-\infty)} Y_1(\xi,t) = 0$$

$$\lim_{t\to(+\infty)} Y_2(\xi,t) = 0 \quad ; \quad \lim_{t\to(-\infty)} Y_2(\xi,t) = 1$$

The solutions can be determined as above and are

$$H(\xi,t) = \frac{H_j}{2}\,\text{erfc}\left(\frac{t}{\sqrt{4\xi}}\right) + \frac{H_e}{2}\left[1 + \text{erf}\left(\frac{t}{\sqrt{4\xi}}\right)\right] \qquad (34)$$

$$-\frac{(H_e - H_w)}{2}\, e^{\left(\frac{A^2\xi}{\Delta} - \frac{At}{\Delta}\right)}\left[1 + \text{erf}\left(\frac{t}{\sqrt{4\xi}} - \frac{A\sqrt{\xi}}{\Delta}\right)\right] \qquad (35)$$

$$Y_1(\xi,t) = \frac{1 + \text{erf}\left(\frac{t}{\sqrt{4\xi}}\right)}{2}$$

$$Y_2(\xi,t) = \frac{\operatorname{erfc}\left(\frac{t}{\sqrt{4\xi}}\right)}{2} \tag{36}$$

Transformation to the Physical Plane

In order to use these solutions to describe a given physical problem, it is necessary to invert the transformations from (y→t), i.e.,

$$y = \int_0^t \frac{\rho_e}{\rho}\, dt' \tag{37}$$

and (x→ξ), Eq. (29). To perform these operations, we must have the local variation of static density. Now for a perfect gas

$$\frac{\rho}{\rho_e} = \frac{W}{W_e}\left(\frac{T_e}{T}\right) \tag{38}$$

so that we require the static temperature. Taking the static temperature - enthalpy relation as locally linear in the vicinity of some reference temperature, T_r, for each constituent, i.e.,

$$h_i = \Delta_i + \bar{c}_{p_i}\,(T - T_r) \tag{39}$$

and noting $h = \Sigma\, Y_i h_i$ and $H \equiv h + u^2/2$ we can finally write

$$T = T_r + \frac{H(t,\xi) - \frac{u_e^2}{2}\left(\frac{u}{u_e}\right)^2 - \Sigma\, Y_i \Delta_i}{\Sigma\, Y_i\, \bar{c}_{p_i}} \tag{40}$$

The required operations were performed numerically on an IBM 7094. These results were then analyzed by computer to determine the streamline and isotherm patterns.

NUMERICAL EXAMPLES

The results of sample calculations display some interesting effects for different cases determined by the initial conditions.

Perhaps the most important case is that where the freestream static temperature is sufficiently low that boundary layer effects must be relied upon to produce ignition in a practical distance. One can easily calculate the maximum static temperature in the boundary layer for a given wall temperature and thence might conclude that ignition could be readily achieved in a given case. The detailed description of this process produced by the present analysis

shows that such an approach is superficial and often misleading. The physical size of the initial splitter place boundary layer plays a dominant role in determining whether ignition will indeed occur regardless of the wall temperature or the maximum temperature in the boundary layer. This point is clearly displayed by numerical results for the typical cases, "A" and "B" in Table I.

TABLE I

Initial Conditions for Numerical Examples

CASE	T_e °K	U_e, fps	T_w, °K	T_{oj}, °K	Δ, ft	P_e, atm
A	750	10,000	300	300	.005	1
B	750	10,000	300	300	.10	1
C	750	10,000	300	500	.10	1
D	750	10,000	300	750	.10	1

The maximum temperature in the boundary layer for either boundary layer thickness would be 1550°K which is certainly high enough to conclude that the wall might cause ignition. The isotherm patterns in the mixing region for the two boundary layer thicknesses are shown in Figs. 7 and 8. The maximum static temperature falls below the auto-ignition level (1000°K) in an axial distance somewhere between one and two initial boundary layer thicknesses in both cases. A conservative estimate of the ignition delay distance for these cases can be made by basing the ignition delay time on the maximum temperature in the initial boundary layer and using the velocity at $T = T_{max}$ as the characteristic velocity. For the conditions of this problem taking the static pressure as one atmosphere[4]

$$\tau_{ig}\ (T_{max}) = 5 \times 10^{-6} \text{ sec.}$$

so that

$$\ell_{id} = \tau_{id} \times u(T_{max}) = .028$$

Thus, for Case "A" (Δ = .005 ft.) the local static temperature is depressed in a distance far too short for ignition by mixing with the colder fuel and from the acceleration due to viscous shear.

The streamline through the maximum temperature in the initial splitter plate boundary layer is also shown in Fig. 7. Observe that it does not follow the region of maximum static temperature as it proceeds downstream. Thus, the maximum temperature in the initial boundary layer is not a reliable index for ignition unless the ignition delay distance based upon it is small compared to the boundary layer thickness. The streamline that passes through the point $T = .8\ T_{max}$ in the region above T_{max} is also shown for reference. It tends

to follow the region of maximum temperature somewhat better but still is not a reliable index for ignition.

In Fig. 8, lines of constant equivalence ratio for two values: $\varphi = 1.0$ ($Y_{H_2} = .0292$) and $\varphi = .10$ ($Y_{H_2} = .00292$) are shown. The lean ignition limit for hydrogen is about $\varphi = .10$ and it can be seen that the line representing this value passes through the region of high static temperature. Again, it is important to note, that this minimum hydrogen concentration does not occur concurrently with T_{max}, further substantiating the assertion that T_{max} alone is not a sufficient gauge of ignition probability. On the basis of these results, we conclude that for the case of cold fuel injection, wall effects cannot be relied upon to produce ignition, unless the boundary layer is at least the order of the ignition delay distance based on T_{max} and $U(T_{max})$. Typical static temperature and velocity profiles at several exit stations are given in Fig. 9 and Fig. 10 for information.

Another interesting consideration is the influence of initial fuel temperature on the foregoing conclusion. To investigate this effect, two additional calculations were made using the same air side conditions but varying the fuel total temperature to 500°K and 750°K with the jet Mach number held at unity. These cases are denoted as "C" and "D" in Table I and the resulting isotherm patterns are given in Figs. 11 and 12. Comparing with Case "B" (same $\Delta = .100$ ft), it can be readily seen that the regions of elevated temperature are extended downstream by the hotter fuel. This is certainly to be expected since the amount of energy involved in hydrogen heated an additional few hundred degrees Kelvin is considerable and the energy exchange that occurs upon mixing with the hotter air causes a much smaller reduction in air temperature. The important result, however, is that the extension of the region with mixture temperatures above the auto-ignition temperature is not drastic. In the 500°K fuel temperature case, it is extended from slightly more than one to almost two boundary layer thicknesses while the 750°K case extends to somewhat more than two. This is a second order effect when compared to the influence of T_{max} on τ_i and thus does not alter the requirement that the boundary layer thickness must be at least of the order of the ignition delay distance for wall effects to be important. Of course, if the fuel temperature is raised above the auto-ignition temperature then, wall effects on the air side will no longer be dominant and the above conclusions are invalid.

Aside from the actual physical size of the initial boundary layer, its character-laminar or turbulent - has a significant influence. In Fig. 13, the isotherm pattern resulting for the conditions of Case "B" but with a laminar initial boundary layer is shown. When compared with Fig. 8 a large difference is apparent. It should be noted that the same value of the transformed boundary layer thickness Δ, does not imply the same value of the actual boundary layer thickness for a laminar and turbulent case. This is a result of the application of Eq. 13, i.e.

$$\Delta = \int_0^{\delta} \left(\frac{\rho}{\rho_e}\right) dy$$

where (ρ/ρ_e) vs. y is not the same for a laminar and turbulent case. In the present instance for $\Delta = .100$ ft, $\delta = .122$ for the turbulent case and $\delta = .171$ for the laminar case. In Fig. 8 and Fig. 13 it can be seen that a laminar initial boundary layer is beneficial as far as ignition is concerned since the initial rate of mixing is lower when compared to the same situation with a turbulent initial boundary layer. This is, in large measure, due to the fact that the initial value of the eddy diffusivity is small in the "laminar" case since there is no contribution of the upstream turbulent as with a turbulent boundary layer. The lines of constant equivalence ratio at values of $\varphi = 0.10$ and $\varphi = 1.0$ are also shown on Fig. 13 so that they too can be compared to the turbulent case in Fig. 8.

Another related situation is that where the free stream static temperature is slightly above the auto-ignition temperature (1000°K), and where the wall and the fuel are cold. It might be expected that the "cold" boundary layer may retard ignition. In principle this is true, however, the physical size of the boundary layer is again a dominant factor. For example, if the boundary layer is several ignition delay distances thick, then fuel and air will not exist together in region at sufficient temperature to produce ignition for some distance downstream. On the other hand, a small boundary layer will have little retarding effect. However, in the case of hydrogen fuel this whole effect is not generally important. This is a result of the extremely low lean ignition limit and extremely high heat of combustion of hydrogen in air. Thus, a mass fraction of hydrogen of only about 0.003 is sufficient to cause the release of significant amounts of heat. This concentration is normally achieved far out in the boundary layer (see Fig. 8) where the static temperature is near the free stream value in a reasonably short distance so that even a large boundary layer would not retard ignition markedly.

In conclusion then, the major result of this study is that the physical size and character of the initial boundary layer play a dominant role in determining whether wall effects can be relied upon to produce auto-ignition in a supersonic stream. No simple exact result has been obtained, but an adequate estimate is contained in the statement that

$$\frac{\delta}{\tau_{id}(T_{max})\ u(T_{max})} > 1$$

for a reasonable expectation of wall effects alone to produce ignition.

COMPARISON WITH EXPERIMENT

The results of the analysis developed in the previous sections can be compared to the experimental observations previously made by the writer, mentioned in the Introduction. First, the general test arrangement is described; then the pertinent experimental results are presented. Finally, analytical predictions for the conditions of the experiment are presented and discussed.

[redacted]

Experimental Apparatus

It is always desirable to formulate an experimental investigation which embodies all the phenomena of interest to the intended application but yet which idealizes the general physical problem in order to increase the likelihood of obtaining an analysis to compliment the experimental data. One variable that greatly complicates any attempt at analyzing the mixing process involved here is the gradient of static pressure. The experimental arrangement used for the studies described in this report was therefore specifically designed to minimize the variation of static pressure throughout the combustion region. At a first glance, the configuration shown in Fig. 14a would seem to be the most desirable from this standpoint as there would be no reflections of the compression waves caused by local streamtube expansion in the reaction zone and any question of thermal choking is circumvented by the large available area. The arrangement shown in Fig. 14b, however, possesses the additional advantage that the tendency toward a general increase in static pressure level along the combustion zone is countered by the expansion waves that are reflected from the free streamline that bounds the air flow. Initially, this streamline is made horizontal by matching the pressures before the step and in the cavity; it then adjusts its direction to maintain constant static pressure along the boundary.

The combustion test chamber is two-dimensional with a slot mounted in the straight wall forming the top of the chamber as shown in Fig. 15. A contoured Mach 2 nozzle is supplied by a combustion fired blow-down air heater shown with the test section mounted at the exit. Air and oxygen are metered in preset proportions into a plenum chamber at the rear; hydrogen is injected around the periphery in the downstream direction by means of a perforated ring and the mixture is ignited by a 15,000 volt spark. The flame and combustion products are confined in a seven inch inside diameter carbon steel pipe five feet long. The hydrogen and oxygen addition to the main air stream are determined to produce a given temperature of the products of combustion and to make up the oxygen consumed in the reaction such that the mass fraction of oxygen in the products is the same as in pure air. Typically, a mixture to produce "vitiated" air at 1400^{o}K will have a mass fraction of oxygen of 0.23, water 0.10 and nitrogen 0.67 as opposed to pure air with a mass fraction of oxygen of 0.23 and nitrogen 0.77. It is believed that this impurity in the main air stream will have a small effect on the chemistry of the ignition process under consideration. The total temperature and pressure of the "air" are monitored and recorded by thermocouples and pressure transducers. The exhaust from the heater is then passed through a two-dimensional throat and expanded to Mach 2 at the injection station. The cross-section of the tunnel at the injection station is a rectangle two inches high and three and one-half inches wide.

Hydrogen for fuel in the test section is heated by a bed of hot stainless steel balls 3/8" in diameter contained in a vertical 3" pipe mounted on the fuel injection block. This heater produces hydrogen at temperatures up to 825^{o}K, which is then exhausted into the main air stream through a wall slot at sonic conditions.

[redacted]

Experimental Results and Interpretation

The first test series was run with a large sonic slot (.310 in.) as shown in Fig. 16. This slot allows injection of amounts of hydrogen fuel up to stoichiometric proportions while matching static pressures at the exit.

Representative photographic results are shown in Fig. 17 for an "air" stagnation temperature of 1670°K and stoichiometric proportions of hydrogen with a stagnation temperature of 450°K. The two pictures given as Fig. 17a and Fig. 17b are luminosity photographs taken with the window in the downstream position and a three probe rake in the flame zone at the exit. The first picture was taken perpendicular to the test section while the second is taken slightly to the rear to allow viewing somewhat into the test section at the end. Two observations are important. First, the flame zone is off the tunnel wall and is located along the interface between the hydrogen and air streams. Secondly, there is a separate flame zone which hangs in the eddy caused by the termination of the top wall of the tunnel which indicates that the injected hydrogen has not been entirely consumed in the chamber length of approximately twelve inches. This result is anticipated on the basis of the non-dimensional length, expressed in slot heights, available for combustion. For the present configuration, this parameter, (L/a), is roughly 40 which is considered short on the basis of the approximate mixing analyses available. This length, while being too short to expect complete combustion, is sufficient for studying the ignition process.

A shadowgraph of the rake in the flame as shown in the luminosity photographs is given as Fig. 17c. Normal shocks standing in front of the probes are visible demonstrating conclusively that the flow in the combustion zone is supersonic. The poor quality of the shadowgraph is caused by the luminosity of the flame itself which could not be completely filtered out.

The effects of air temperature on the flow field for a given hydrogen fuel temperature were systematically studied, and the important results can be demonstrated by considering two cases having air temperatures of 1500°K and 1670°K with a hydrogen temperature of 780°K and $\varphi = 3/4$. Figure 18 shows the flame pattern for the latter case with a five probe rake in measuring position. The distribution of static pressure along the upper wall of the chamber is given in Fig. 16. A slight compression due to combustion can be observed just downstream of the injection st·tion; this is followed by an expansion which is caused by the reflection of the injection oblique shock from the free streamline at the bottom. A shadowgraph showing this shock and part of the reflection region for a somewhat higher equivalence ratio ($X = 1.0$) is shown in Fig. 15. The flow is from left to right and the end of the contoured nozzle is visible at the bottom of the photograph. The vertical disturbance at the extreme right hand side of the picture is a stagnation region caused by the fact that the window itself is recessed 1/16" from the tunnel surface.

For this particular case, the Mach number behind the shock is approximately 1.7; of course, the flow is re-expanded to roughly Mach 2.0 by the reflection. Compression from the continuing combustion cancels the expansion along the top wall yielding a reasonably flat pressure distribution for the remainder of the test section. The rake at the exit measured five pitot pressures at the locations shown in Fig. 16; by assuming a value for the ratio of specific heats and a static pressure of one atmosphere, a Mach number distribution can be determined. An estimate of real gas and composition effects shows that a constant value of $\gamma = 1.20$ closely simulates the real physical processes for the purposes of calculating Mach number. A distribution obtained in this way is given in Fig. 20 which again shows the flow to be supersonic in the flame. The wall temperature was measured as 755°K which results in a maximum static temperature of 1100°K in the air boundary layer approaching the injection station.

Lowering the air stagnation temperature to 1500°K for the same hydrogen conditions results in the flame pattern shown in Fig. 21, where the flame emerges as a large bushy jet. The top wall static pressure distribution obtained under these conditions is shown in Fig. 22. It is important to note that there is no initial compression and that the expansion is more severe than in the previous case indicating that there was no combustion and hence no compression before roughly six inches. Beyond this point, combustion begins but in a region where the gases have become well-mixed. The strong pressure rise that results from such a process cannot be supported by the boundary layer, and the flow separates from the wall causing a strong shock in the stream after which the flow completely breaks down emerging as shown in the photograph. The pitot probes at the exit read roughly atmospheric confirming that the flow had indeed separated resulting in a large recirculation zone. The wall temperature was 820°K which results in a maximum initial air static temperature of 1010°K which is barely the level which is generally accepted as necessary for repeatable auto-ignition and thus results in long delay distances.

Analytical Results for Test Conditions

The test conditions for the higher air temperature (1670°K) test were translated into input conditions for the analysis presented in Sect. 2 and a calculation performed. This test was selected for study since supersonic ignition was achieved in a distance far shorter than would be expected from the free stream conditions, implying that the wall favorably affected the ignition process. On the basis of a simple kinetics approach, a free stream static temperature of 978°K at one atmosphere should result in an ignition delay of 1.5×10^{-4} sec.[4] With a free stream velocity of 4260 fps, this results in an ignition delay length of .63 ft. Furthermore, a recent study[16] indicates that the common chemical kinetics analyses such as Ref. 4 cannot be directly extended in use below 1000°K and that ignition delay times determined in that way are too short. On the basis of all this then, an ignition delay distance of 7 to 8 inches would be expected for the free stream conditions of this test. In the actual experiment, however, a luminous frame was observed

to occur about 2 inches from the injection station indicating that the splitter plate boundary layer must have accelerated ignition. An ignition delay time based on the maximum temperature in the air boundary layer is 6.5×10^{-5} sec. Taking the velocity at the point where the temperature is the maximum as 2754 fps gives an ignition delay distance of .18 ft which is in rough agreement with the experimental result.

One aspect of the initial conditions pertinent to the test requires further consideration and that is whether the initial boundary layer is laminar or turbulent. Since the injection slot is located along the flat surface of a two-dimensional half-nozzle, the upstream run corresponds roughly to a flat plat at the exit Mach number. The Reynolds number based on axial length calculated in this manner is 2×10^6, and with the strongly cooled wall conditions of the test, this should be well in the laminar regime.[7] Furthermore, since what pressure gradient does exist on this surface is favorable, this conclusion is given additional support.

The results of the calculation are most clearly displayed as static temperature profiles at several axial stations as shown in Fig. 23. The solid line is the initial temperature distribution which shows a maximum of 1060°K at a height of .001 ft., the free stream static temperature level of 980°K and the fuel static temperature of 650°K. The dash-dot line is the predicted profile at .02' (roughly 10 δ) downstream of injection. The profile still displays a maximum but the level has dropped to 985°K. As we proceed further downstream the maximum disappears and profiles such as shown for x = .05 and .15 feet are obtained. The positions where an equivalence ratio of one tenth (the lean ignition limit at room temperature) is obtained is shown as a large dot on each profile.

Some observations relative to the ignition question can be readily made. First, while the elevated temperature region due to the initial boundary layer persists for a large distance downstream in terms of boundary layer thicknesses (roughly 10), it is a small distance in terms of the ignition delay distance based in T_{max}. Second, the free stream temperature of the test is so close to the usual 1000°K auto-ignition limit that a not unreasonable error in temperature measurement could confuse the interpretation of the results. It is, therefore, difficult to assert conclusively that this comparison between theory and experiment provides an absolute corroboration of the theory. However, it appears clear that the wall effects must have accelerated ignition and that the analytical results certainly indicate that such effects could have done so for the test conditions. This last statement is necessarily equivocal since it is not possible to assess quantitatively the effects of a gradual streamwise reduction in local static temperature from T_{max} on the ignition process without a chemical kinetics treatment. This is all the more true in the critical region near 1000°K.

CONCLUSIONS

The complicated question of initial air side boundary layer effects on the ignition of slot-injected gaseous hydrogen by a hot air stream has been considered by means of an approximate analysis. The principle effects treated were fuel temperature, boundary layer size and boundary layer character-laminar or turbulent. The regime of conditions where this work is of importance is where the free stream static temperature is low enough that wall effects are the only and thus dominant ignition process. In this case, it is shown that the actual size of the initial boundary layer is all important in that an insufficient size will not produce ignition regardless of the wall temperature, fuel temperature or boundary layer character. A rough rule that the boundary layer be larger than the product of the ignition delay time based on T_{max} and the local velocity at that point provides an estimate of the required scale for a given problem. Of course, the actual free stream temperature, the fuel temperature and the character of the boundary layer must be considered in detail in order to provide a definitive answer.

The analysis was also compared to some previous experimental observations and found to be in general agreement although the conditions of the test were such that a truly definitive corroboration of the analysis was not possible. However, this comparison provides strong evidence for the general adequacy of the theory and it is felt that a useful tool for predicting ignition behavior of suggested systems has been developed.

REFERENCES

1. Ferri, A., "Review of Problems in Application of Supersonic Combustion", Seventh Lancaster Memorial Lecture, London, England, May 1964.

2. Avery, W. H., and Dugger, G. L.,"Hypersonic Airbreathing Propulsion", Astronautics and Aeronautics, June 1964.

3. Dugger, G. L., "Comparison of Hypersonic Ramjet Engines with Subsonic and Supersonic Combustion", 4th AGARD Combustion and Propulsion Coll., Milan, Italy, May 1960, Pergamon Press, 1961.

4. Libby, P. A., Pergament, H., and Bloom, M. H., "A Theoretical Investigation of Hydrogen-Air Reactions" Part I: Behavior with Elaborate Chemistry General Applied Sciences Laboratory, TR-250, August 1961.

5. Westenberg, A. A., "Hydrogen-Air Chemical Kinetics Calculations in Supersonic Flow", Applied Physics Laboratory, CM-1028, December 1962.

6. Schetz, J. A., "The Diffusion and Combustion of Slot Injected Gaseous Hydrogen in a Hot Supersonic Air Stream", Bumblebee Design Panel Meeting, McDonnell Aircraft Co., St. Louis, Mo., Nov. 1963, CONFIDENTIAL.

7. Schlicting, H., Boundary Layer Theory McGraw Hill Book Co., New York, Fourth Edition, 1960, pp. 341-346.

8. Schetz, J. A., "Supersonic Diffusion Flames", AGARD Combustion and Propulsion Collo., London, England, April 1963, also appears in Supersonic Flow, Chemical Behavior and Radiative Transfer, Pergamon Press, London, 1964.

9. Marble, F. E. and Adamson, T. C. Jr., "Ignition and Combustion in a Laminar Mixing Zone", Journal Aero. Sci., April 1964, pp. 85-94.

10. Ferri, A., Libby, P. A., and Zakkay, V., "Theoretical and Experimental Investigation of Supersonic Combustion", Third Int. Congr. ICAS, Stockholm, Sweden, Aug. 1962.

11. Marquardt Corp., TMC Report PR 297-2Q, Second Quart. Prog. Rept., Air Force Contract No. AF 33(657)-8431, 1963.

12. Schlicting, H., Boundary Layer Theory, McGraw-Hill Book Co., New York, Fourth Edition, 1960, pp. 598-600.

13. Clauser, F. H., "Turbulent Boundary Layers", in Advances in Applied Mechanics, Vol. IV, Academic Press, New York, 1956, pp. 2-51.

14. Schetz, J. A., and Jannone, J., "A Study of Linearized Approximations to the Boundary Layer Equations" to be printed in the Journal of Applied Mechanics.

15. Carslaw, H. S. and Jaeger, J. C., Conduction of Heat in Solids, Oxford Univ. Press, London, Second Edition, 1959.

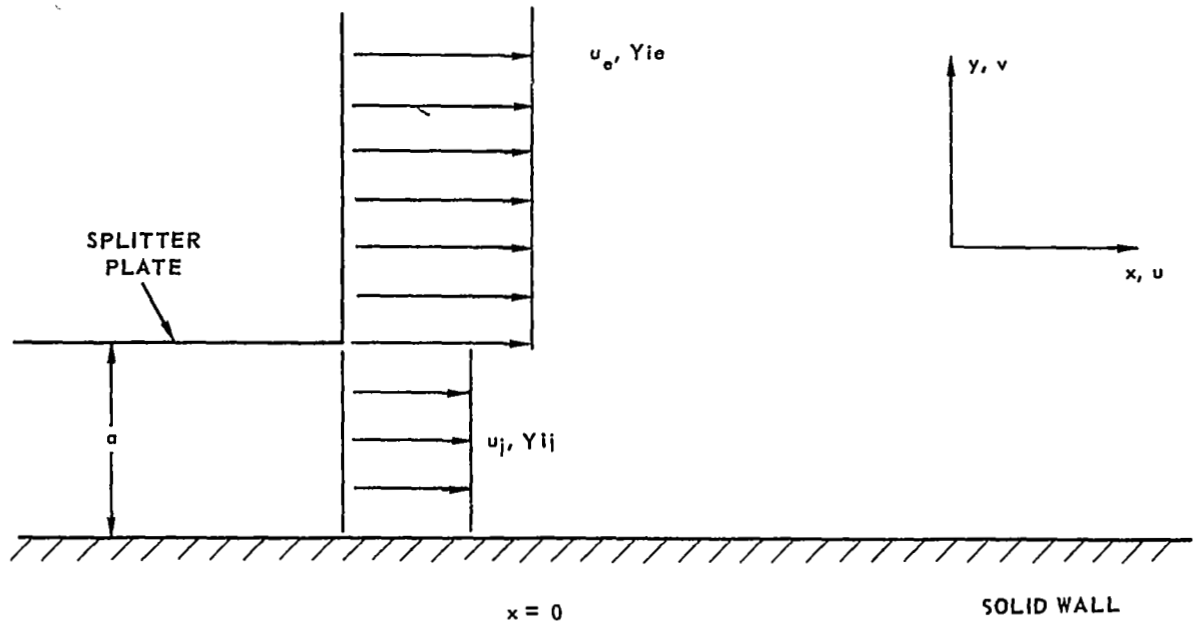

Fig. 1 SCHEMATIC REPRESENTATION OF FLOW FIELD

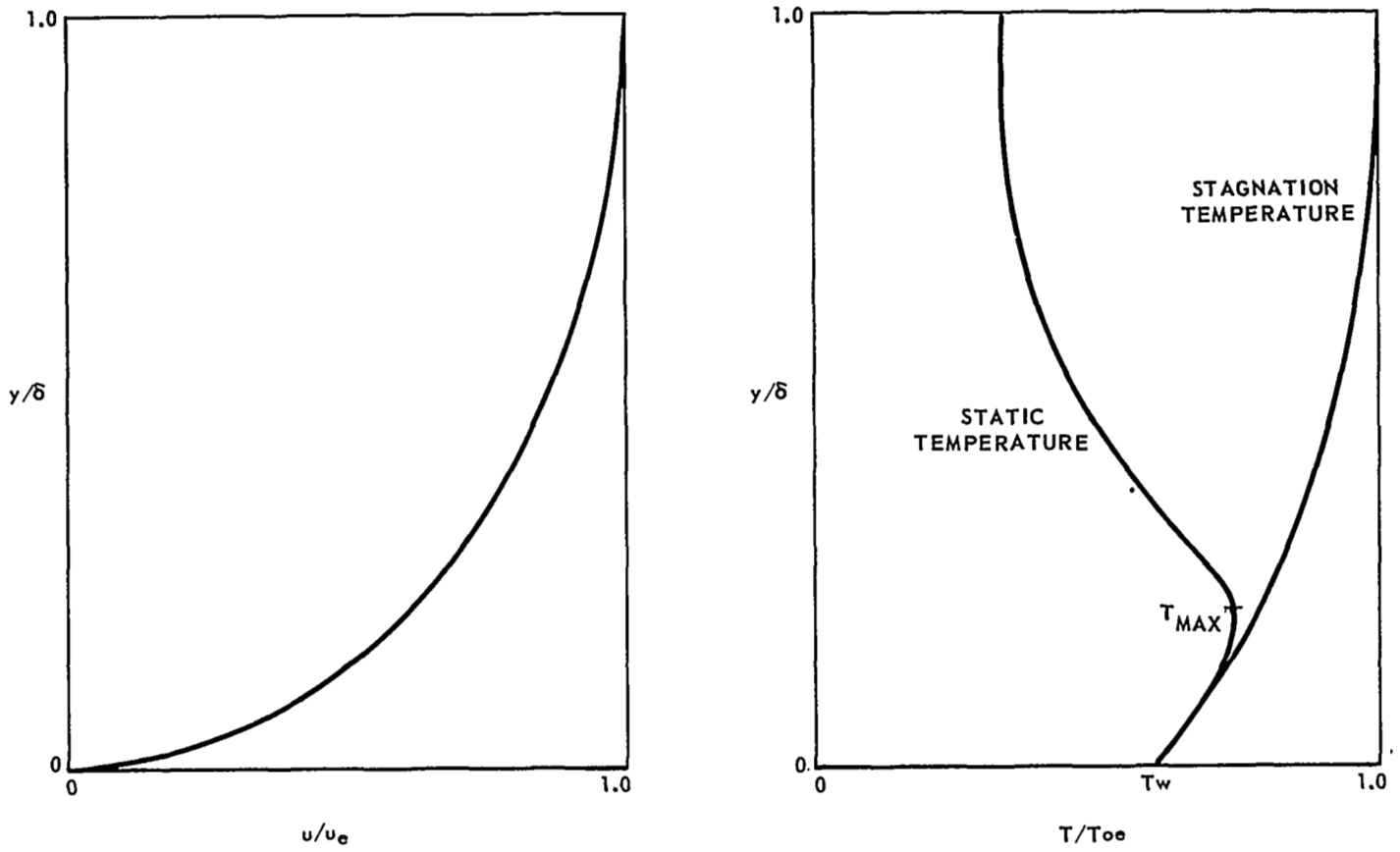

Fig. 2 TYPICAL BOUNDARY LAYER PROFILES IN A SUPERSONIC STREAM

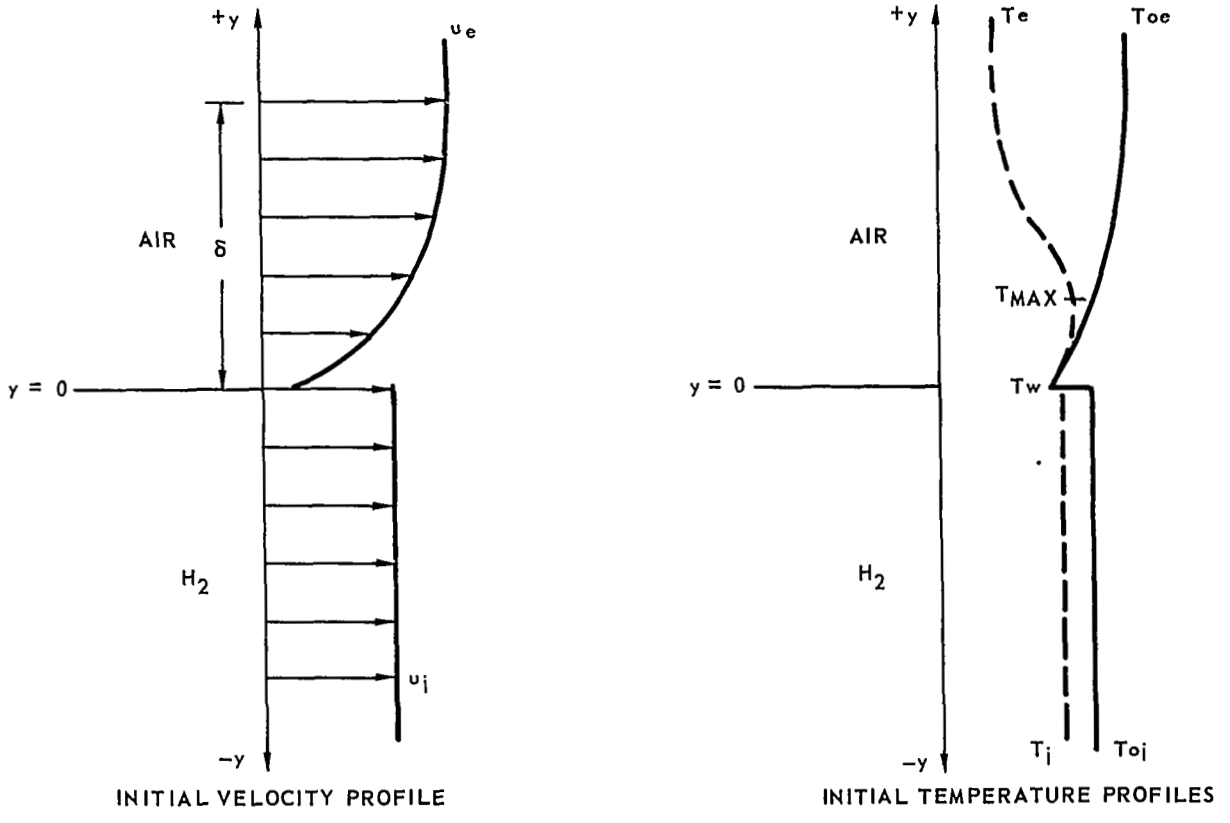

Fig. 3 SCHEMATIC REPRESENTATION OF INITIAL PROFILES USED IN THE ANALYSIS

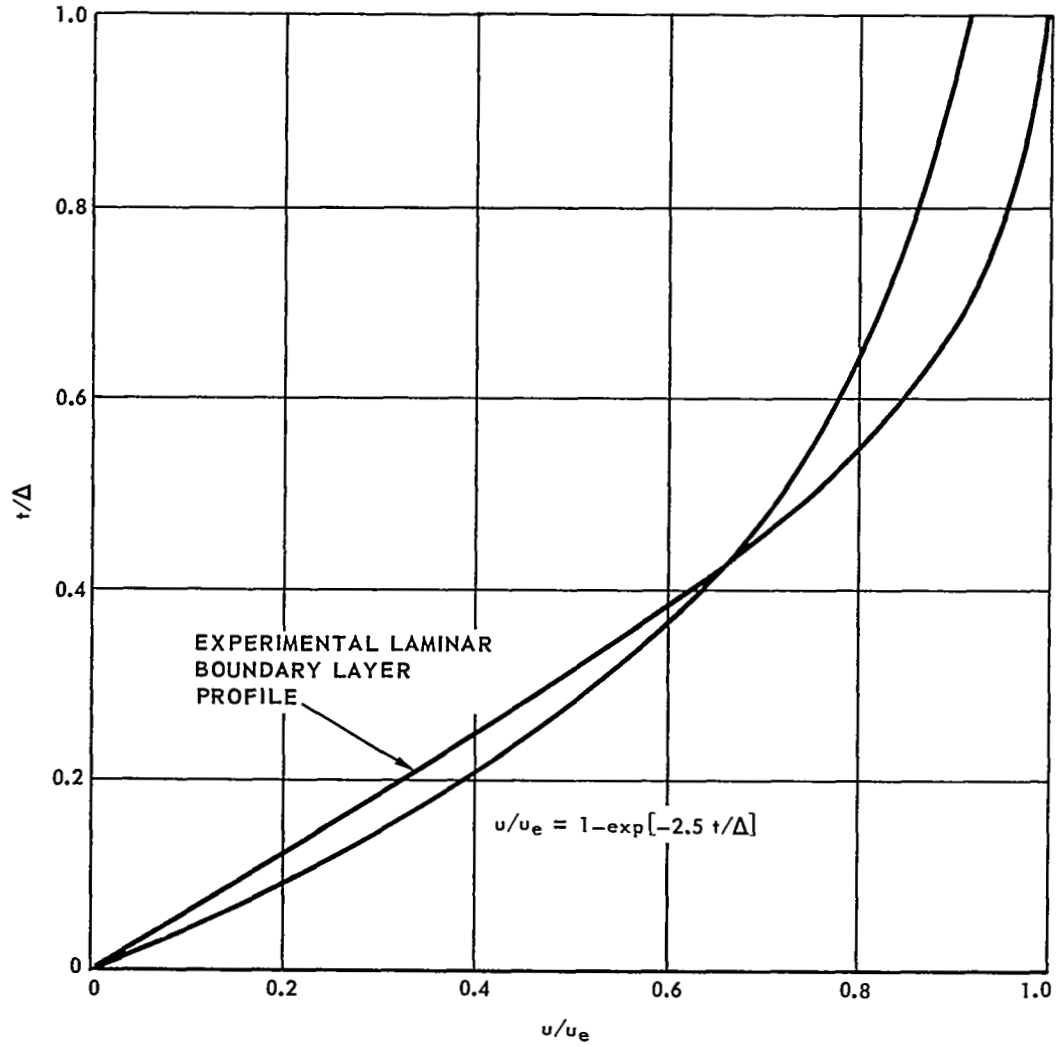

Fig. 4 COMPARISON OF EXPERIMENTAL AND ASSUMED LAMINAR BOUNDARY LAYER PROFILES

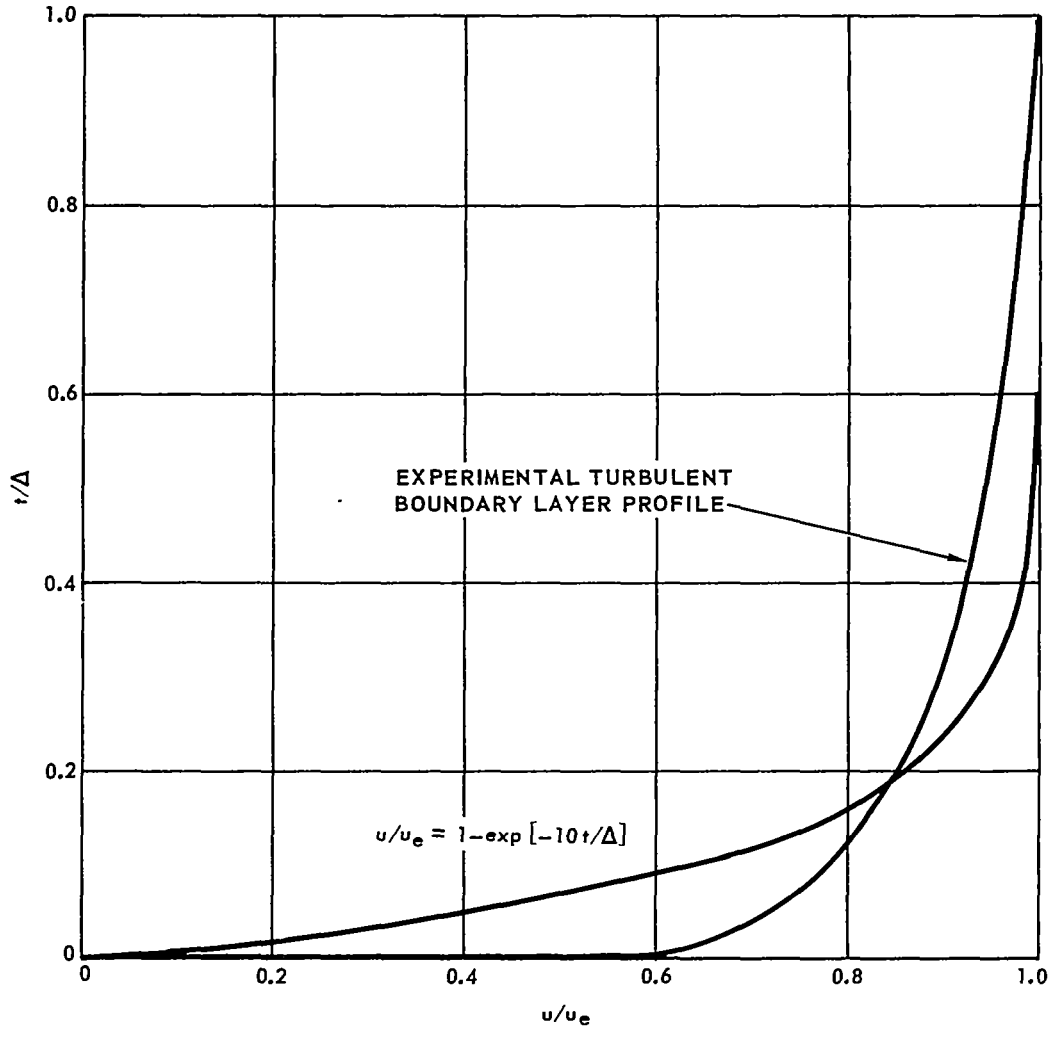

Fig. 5 COMPARISON OF EXPERIMENTAL AND ASSUMED TURBULENT BOUNDARY LAYER PROFILES

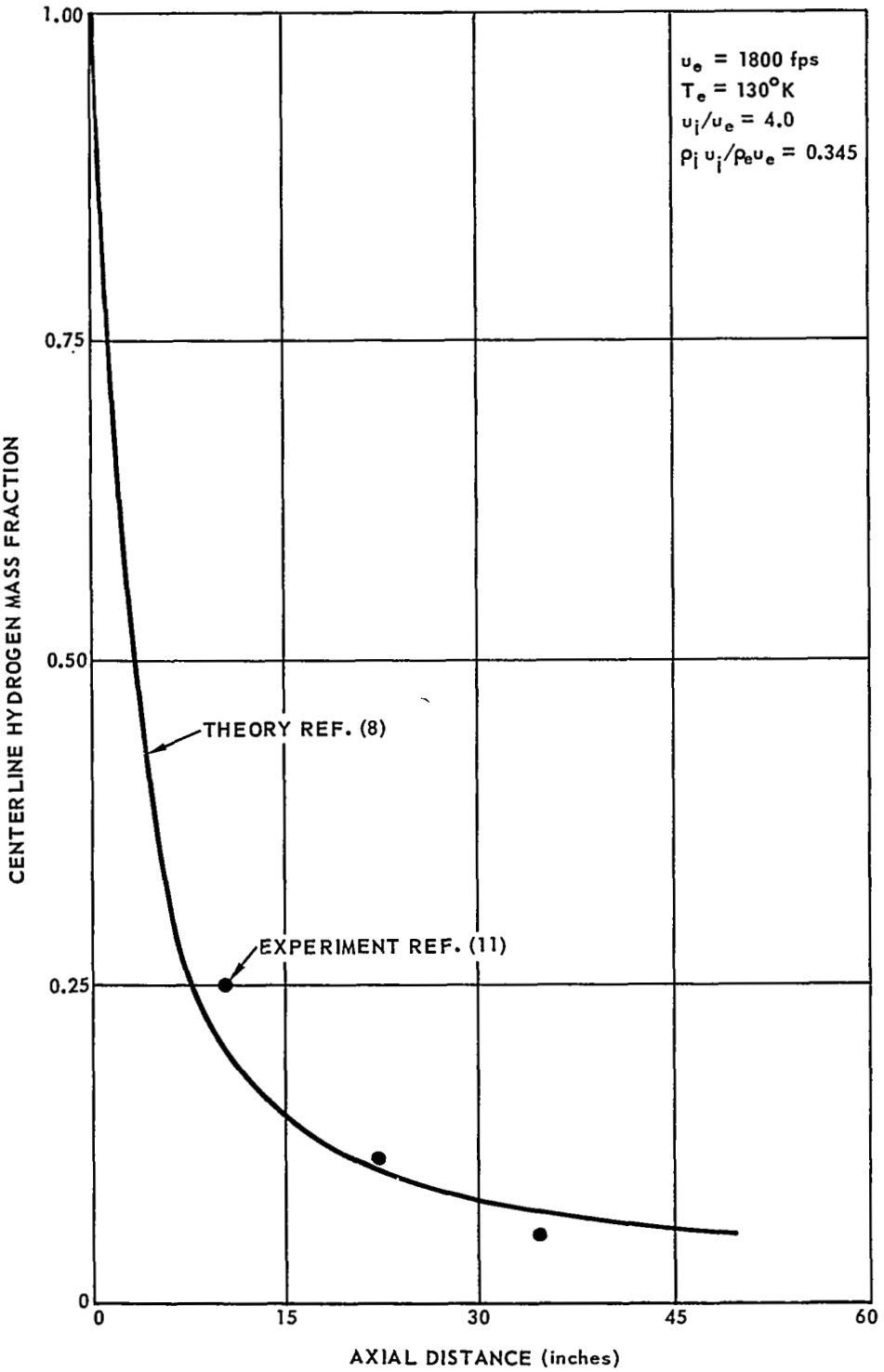

Fig. 6 COMPARISON OF THEORETICAL AND EXPERIMENTAL CENTERLINE CONCENTRATION

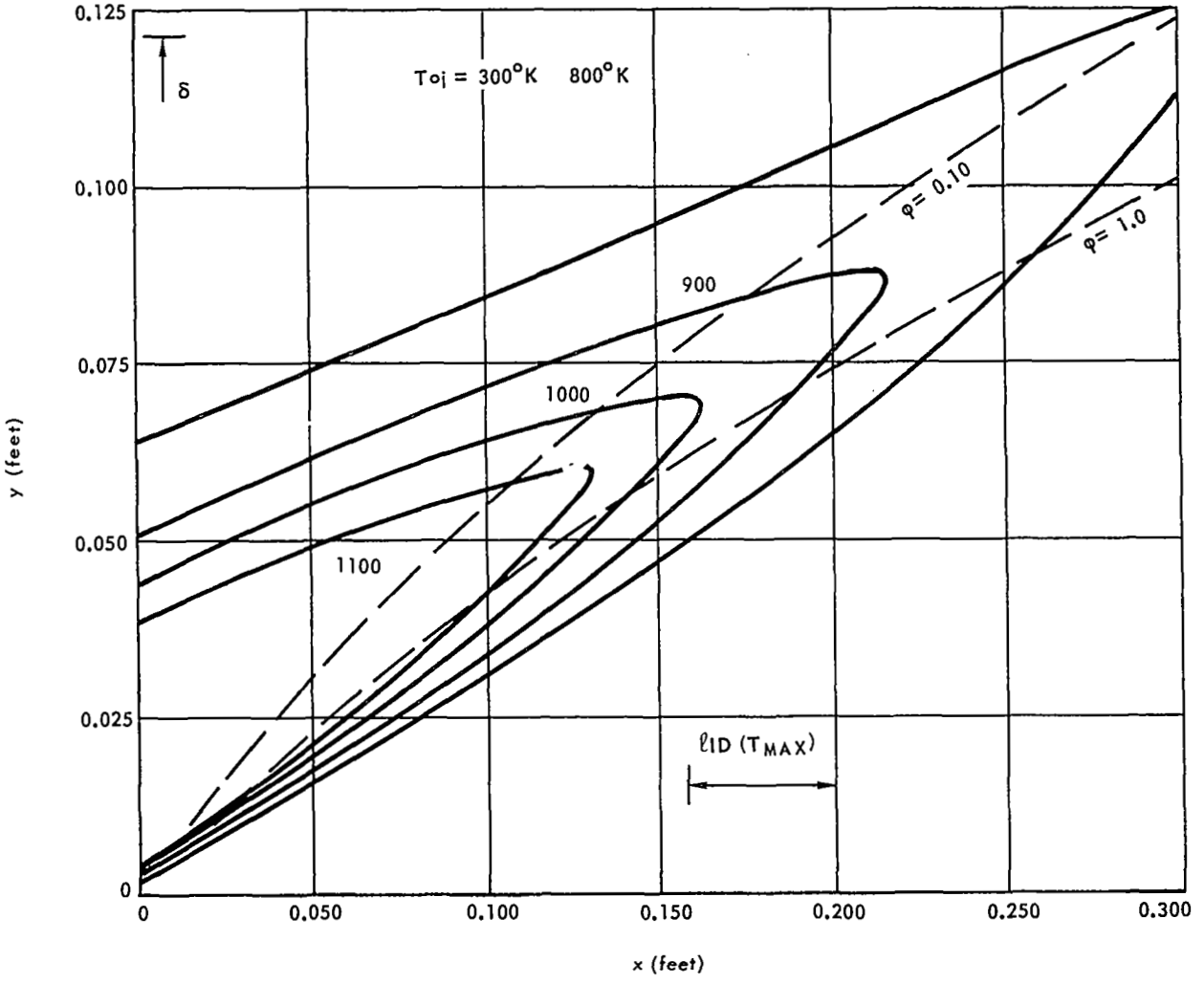

Fig. 7 ISOTHERM PATTERN, CASE "B" (TURBULENT INITIAL BOUNDARY LAYER).

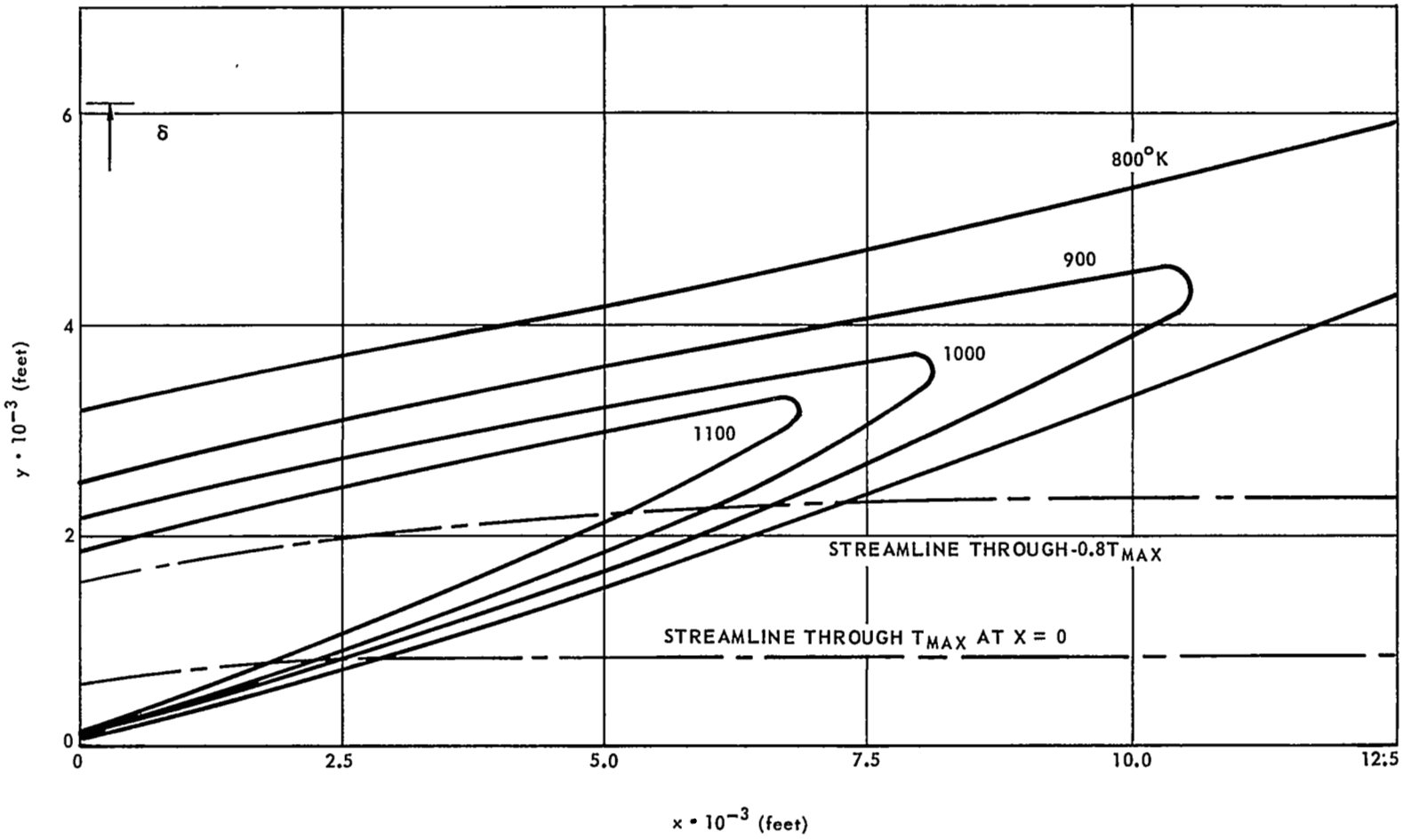

Fig. 8 ISOTHERM PATTERN, CASE "A" (TURBULENT INITIAL BOUNDARY LAYER)

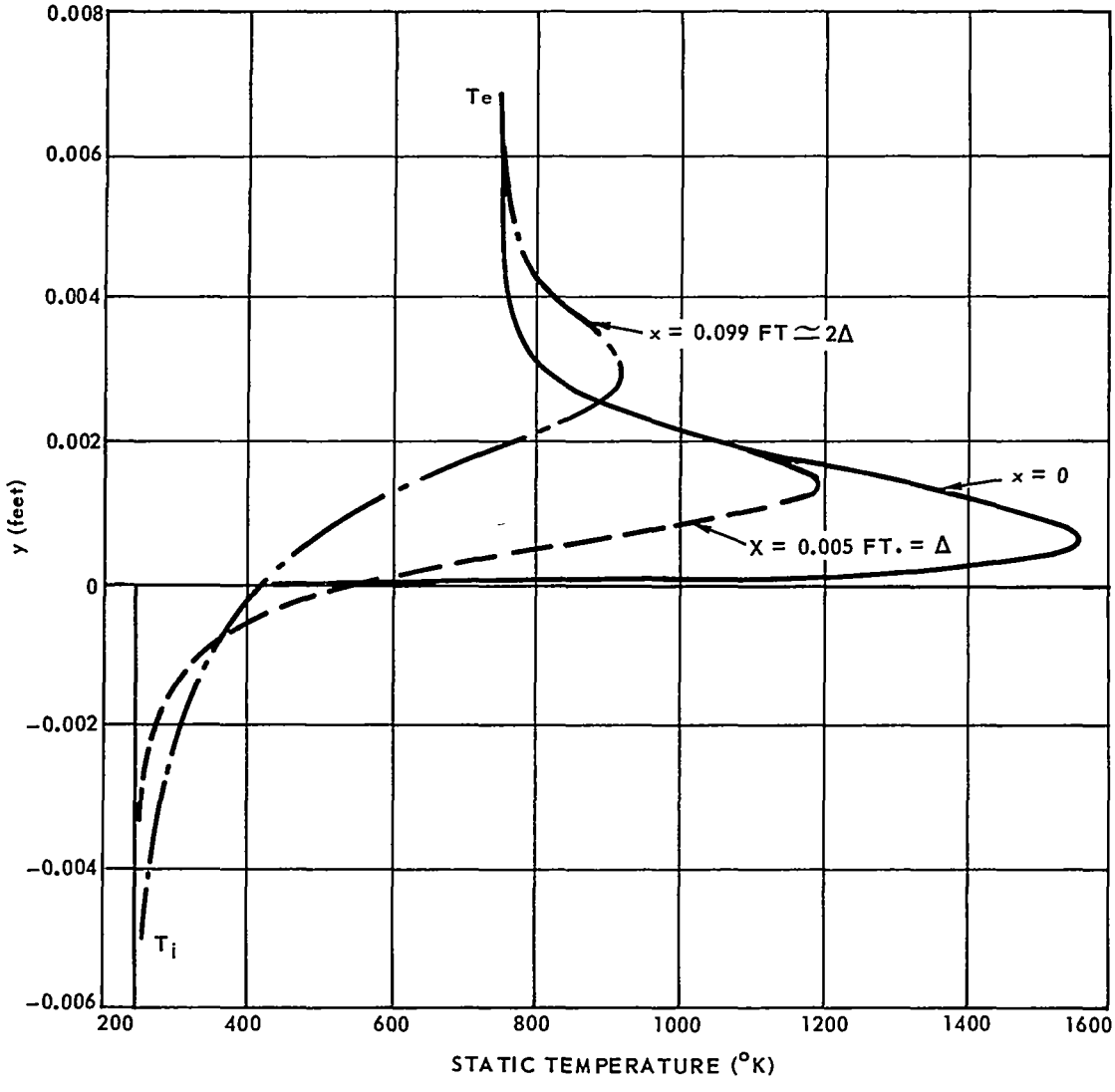

Fig. 9 STATIC TEMPERATURE PROFILES AT SEVERAL AXIAL STATIONS, CASE "A" (TURBULENT INITIAL BOUNDARY LAYER)

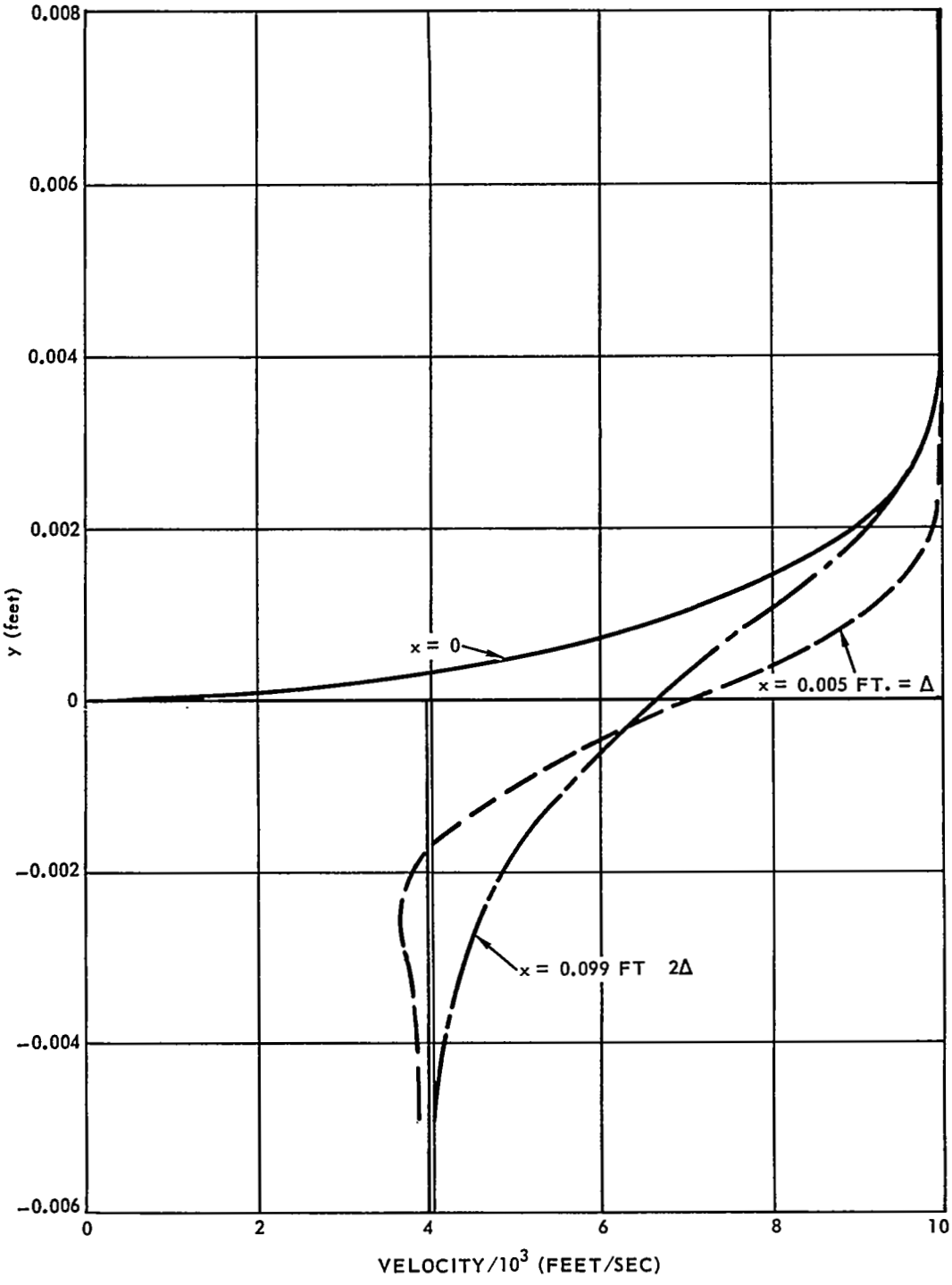

Fig. 10 VELOCITY PROFILES, CASE "A" (TURBULENT INITIAL BOUNDARY LAYER)

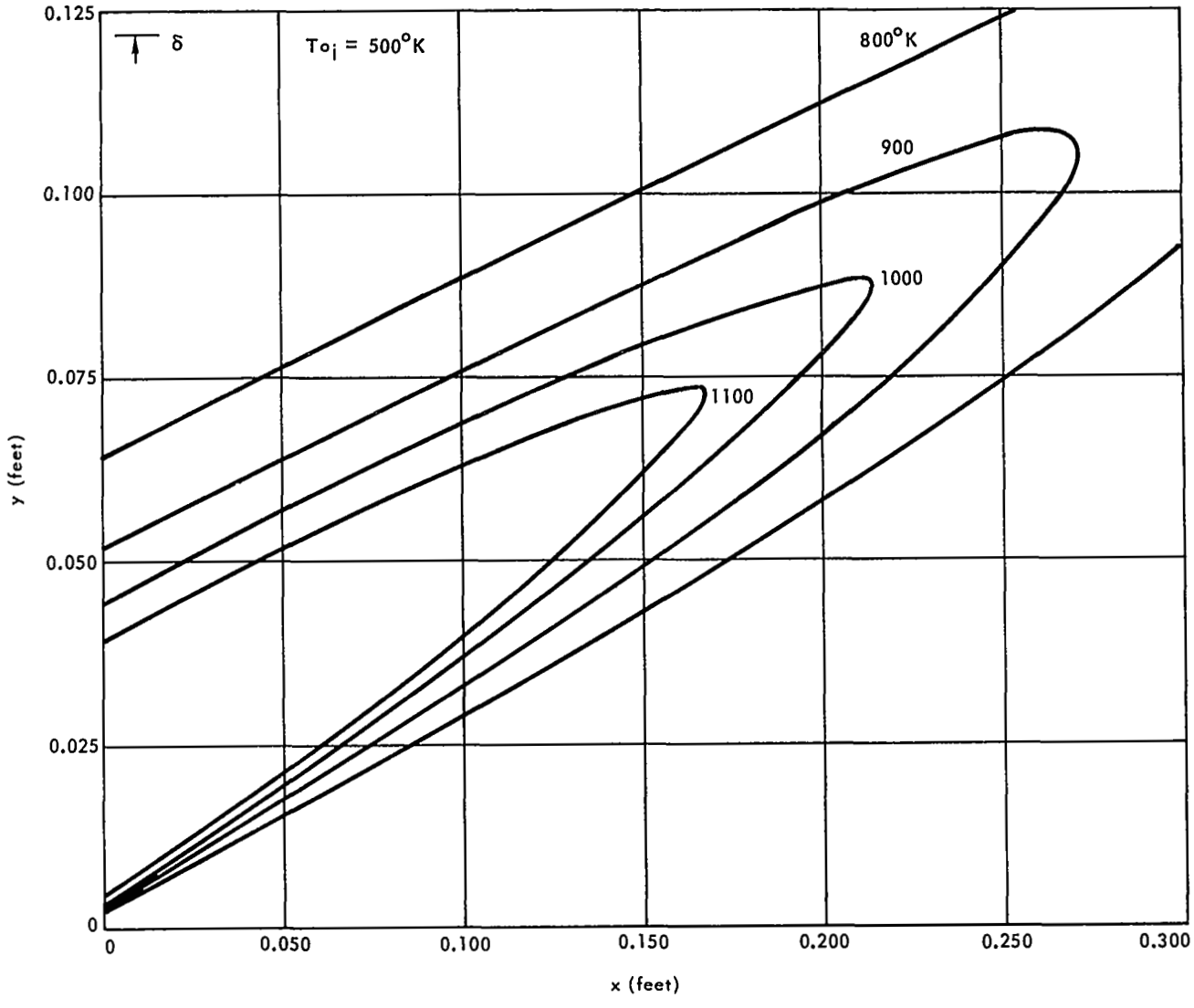

Fig. 11 ISOTHERM PATTERN, CASE "C" (TURBULENT INITIAL BOUNDARY LAYER)

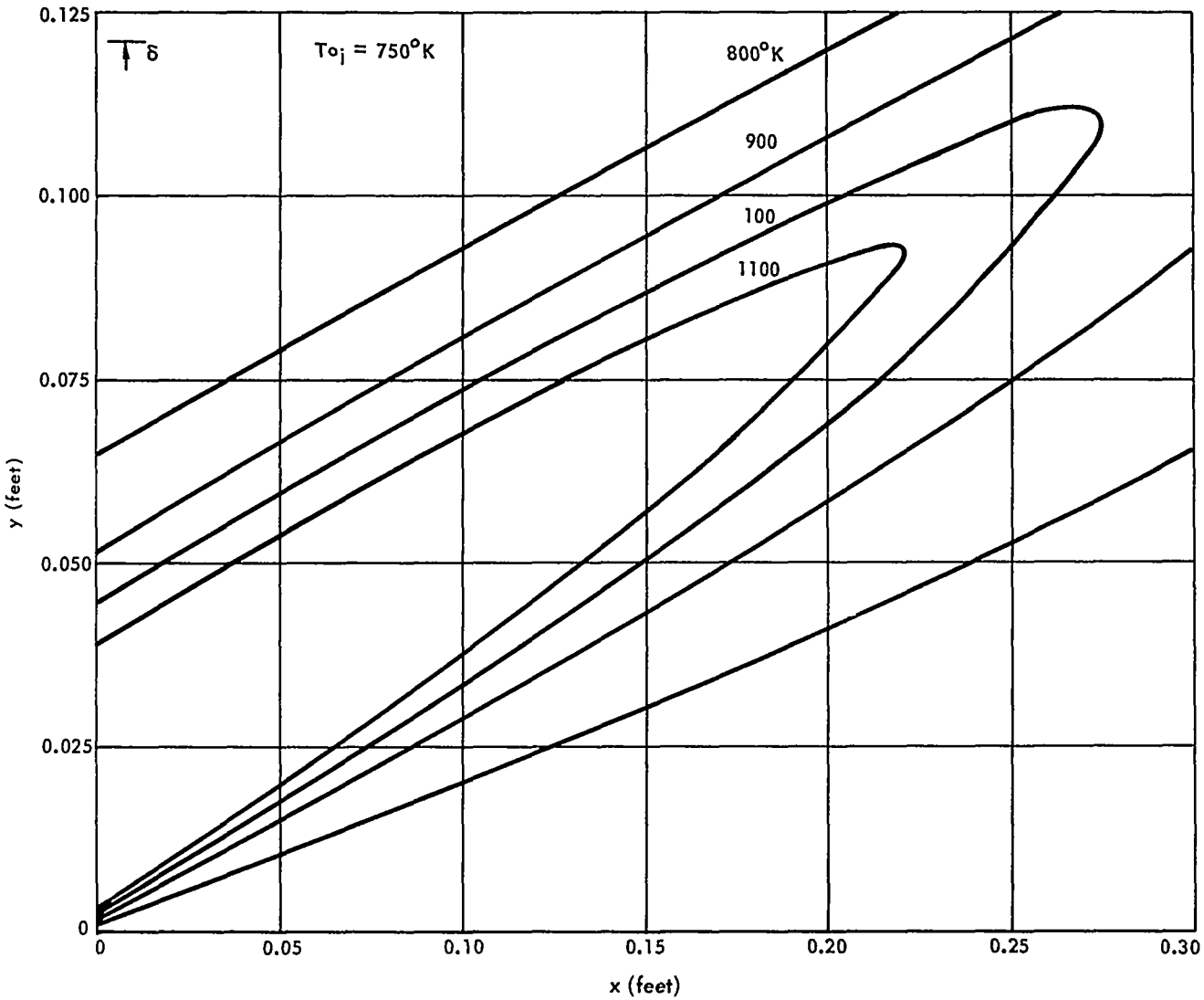

Fig. 12 ISOTHERM PATTERN, CASE "D" (TURBULENT INITIAL BOUNDARY LAYER)

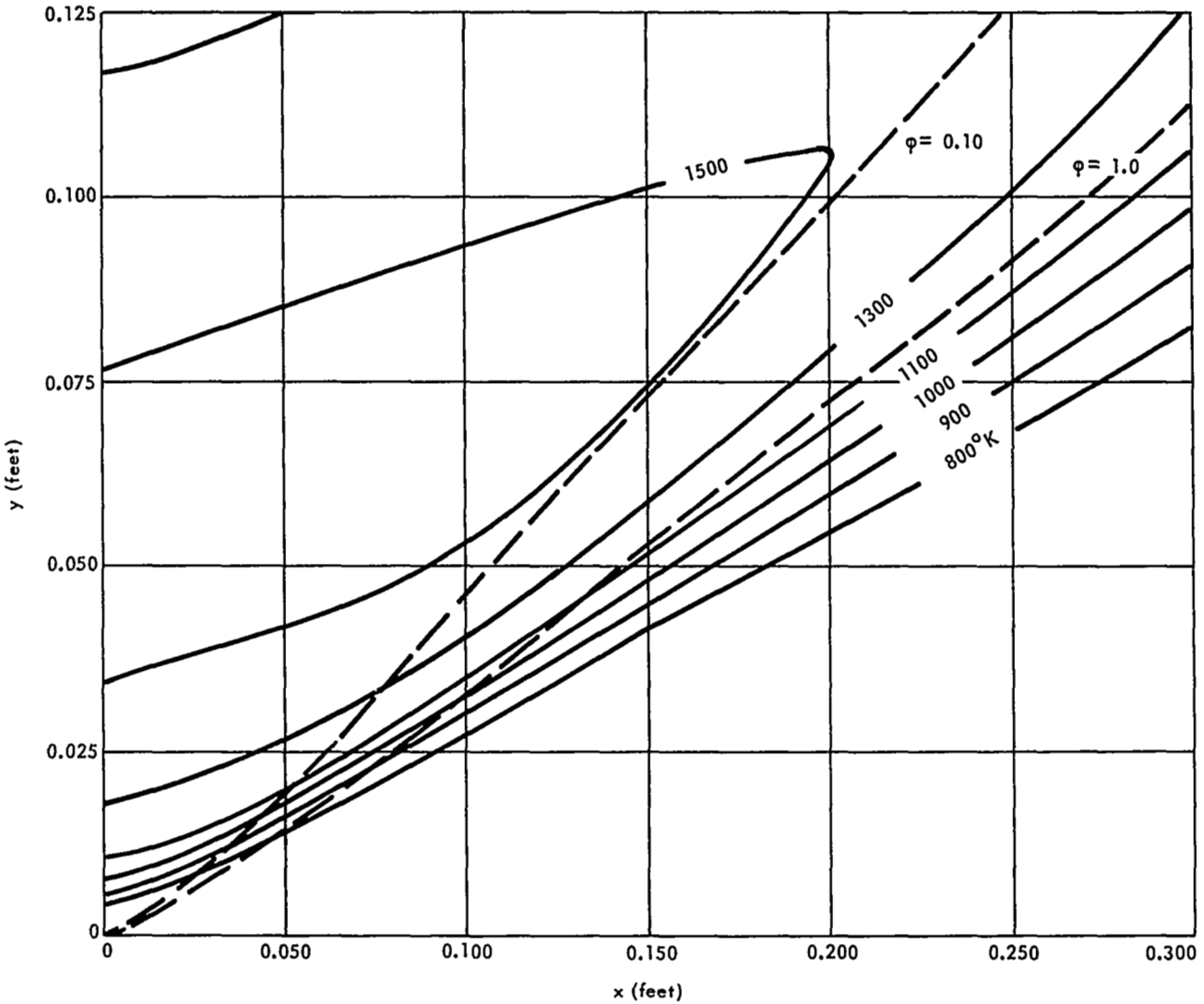

Fig. 13 ISOTHERM PATTERN, CASE "B" (LAMINAR INITIAL BOUNDARY LAYER)

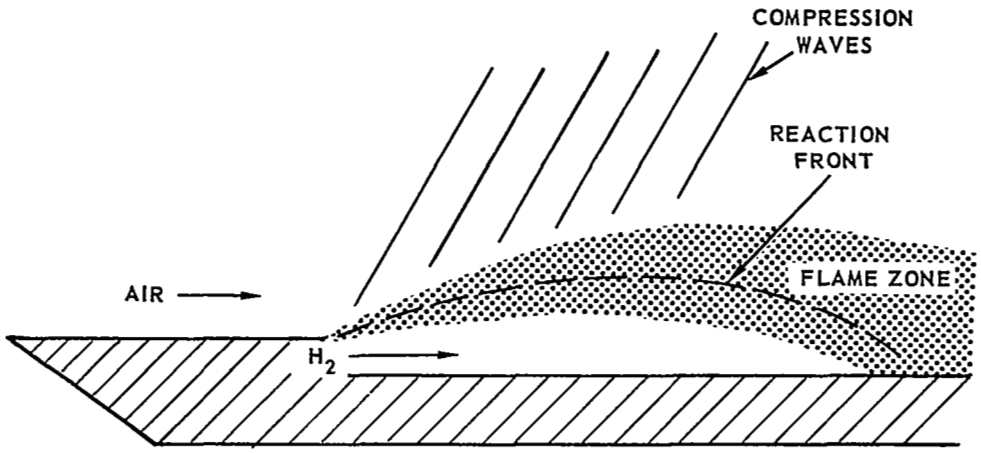

(a) FLAT PLATE IN AN INFINITE STREAM

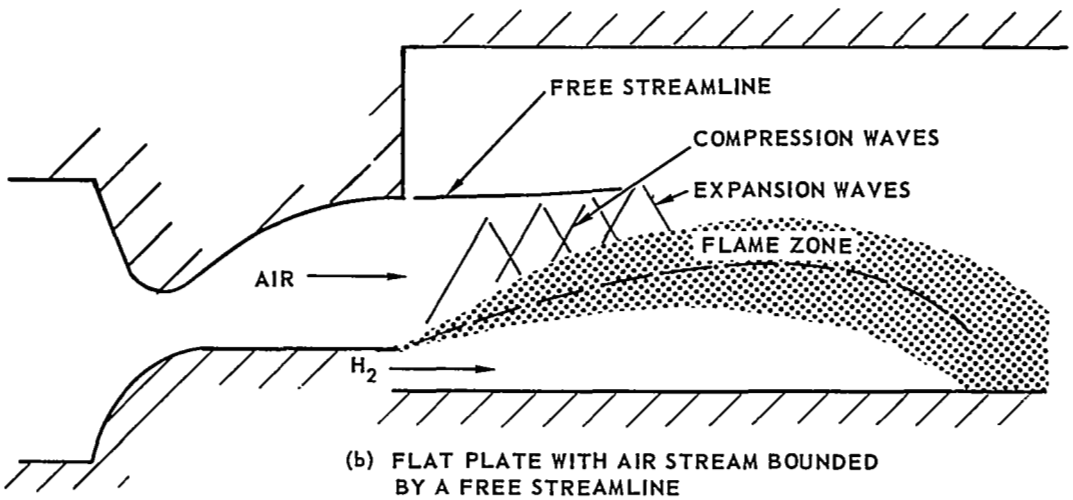

(b) FLAT PLATE WITH AIR STREAM BOUNDED BY A FREE STREAMLINE

Fig. 14 WALL SLOT TEST CONFIGURATIONS

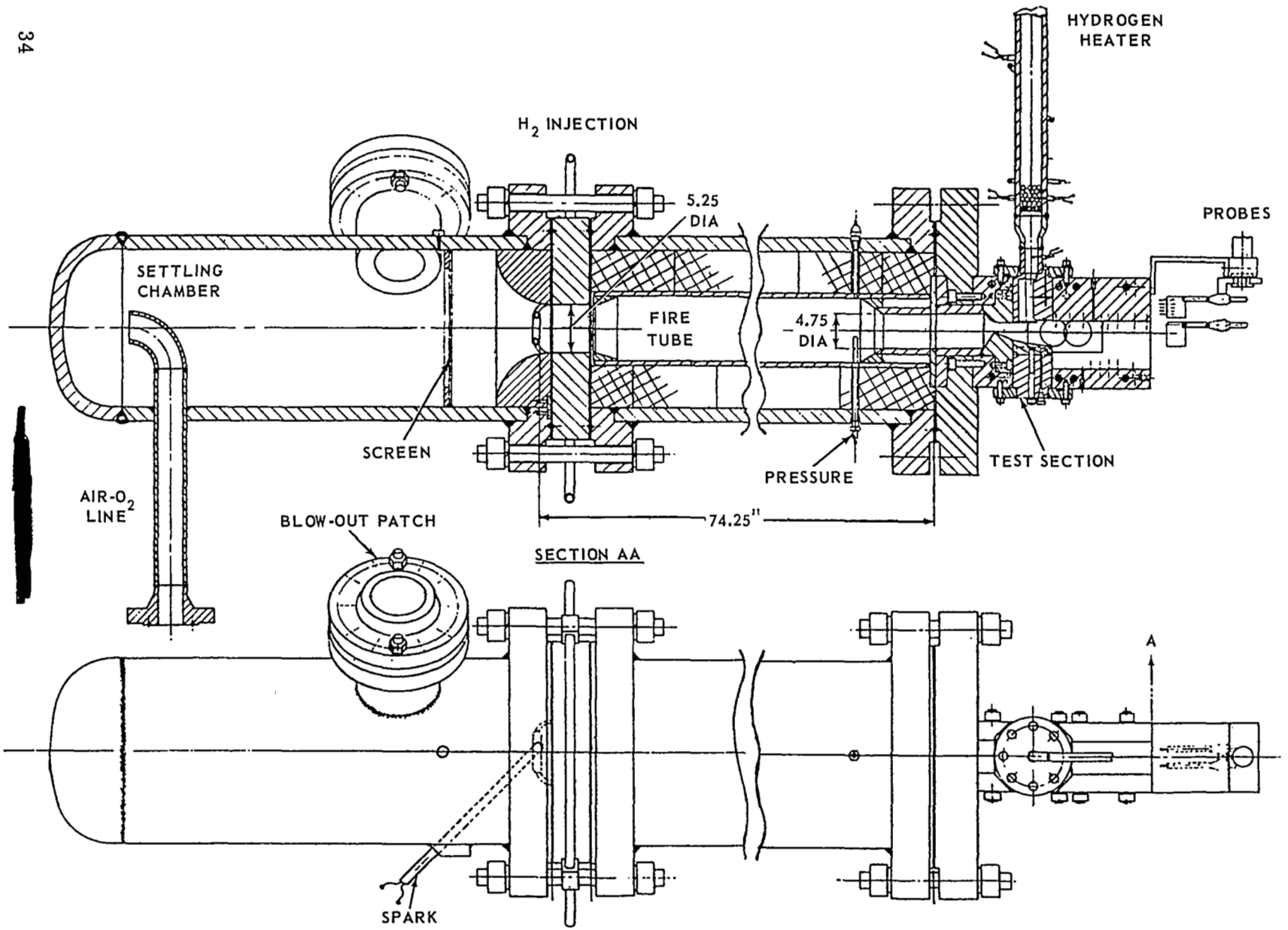

Fig. 15 DETAILS OF EXPERIMENTAL ARRANGEMENT

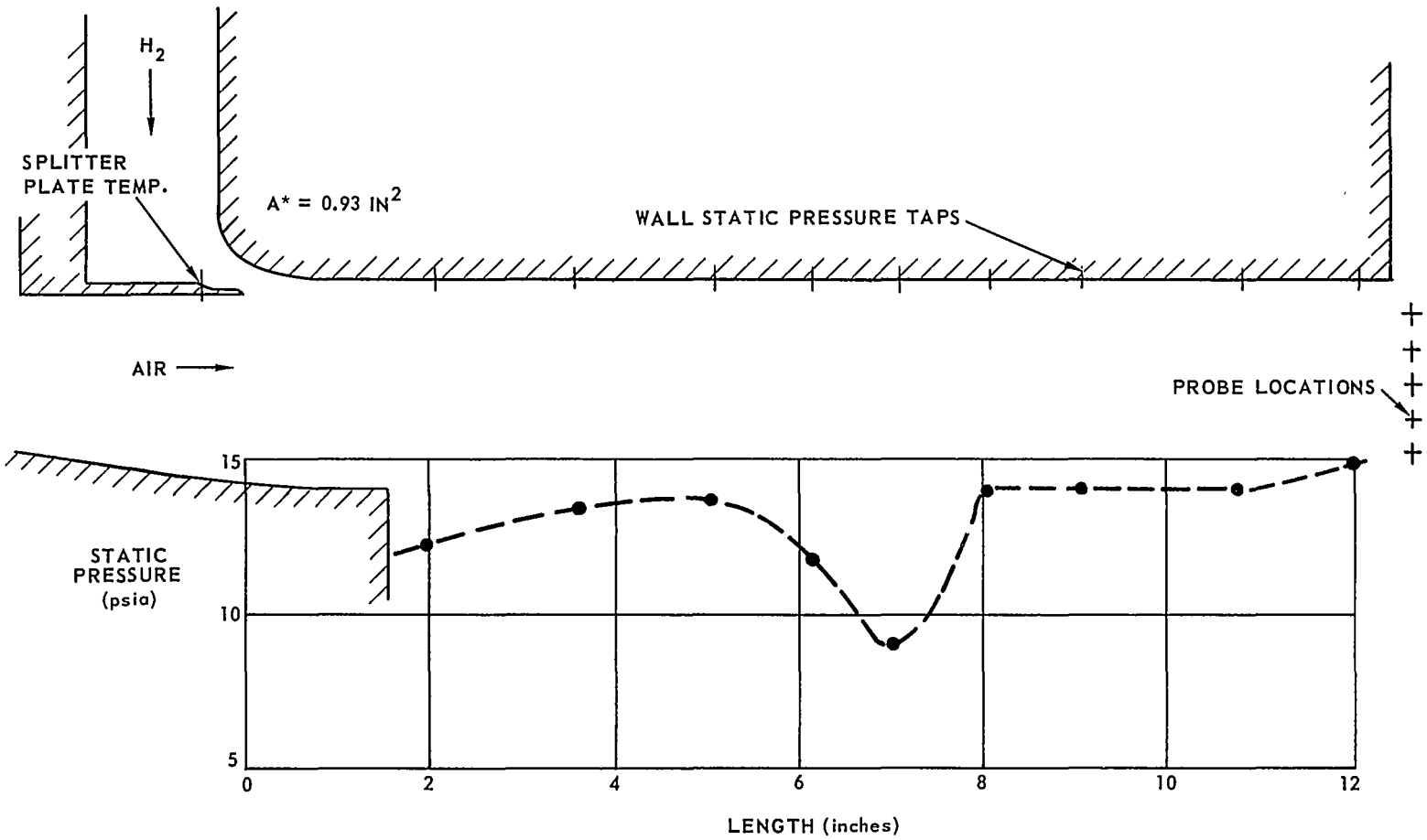

Fig. 16 STATIC PRESSURE DISTRIBUTION –To, AIR = 1670°K, To, H_2 = 780°K, φ = 0.75

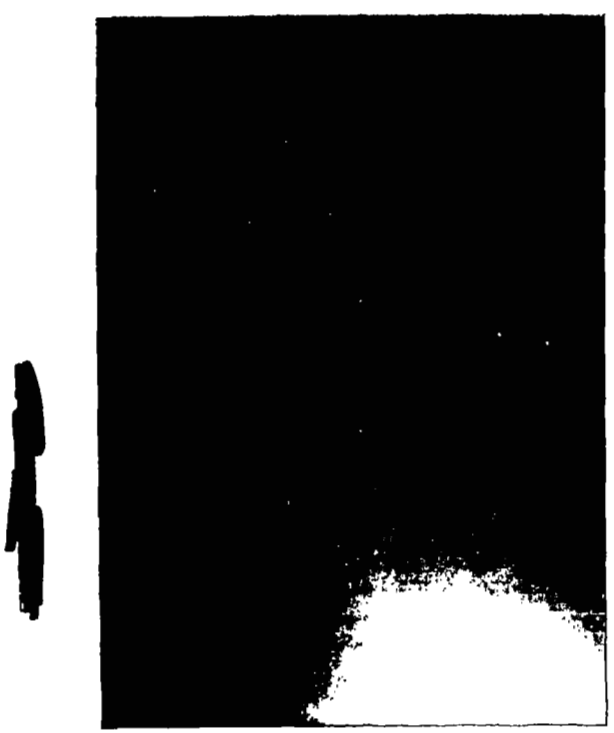

(c) Shadowgraph of the three-probe rake in the combustion zone.

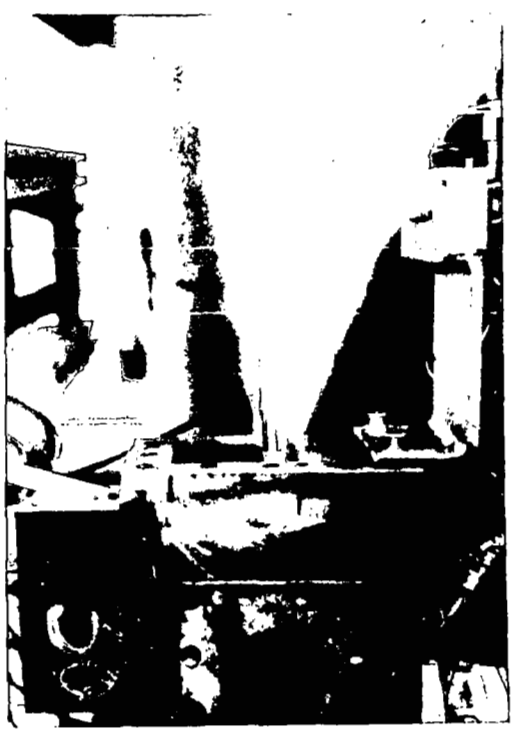

(b) Luminosity photograph from a slight rearward angle.

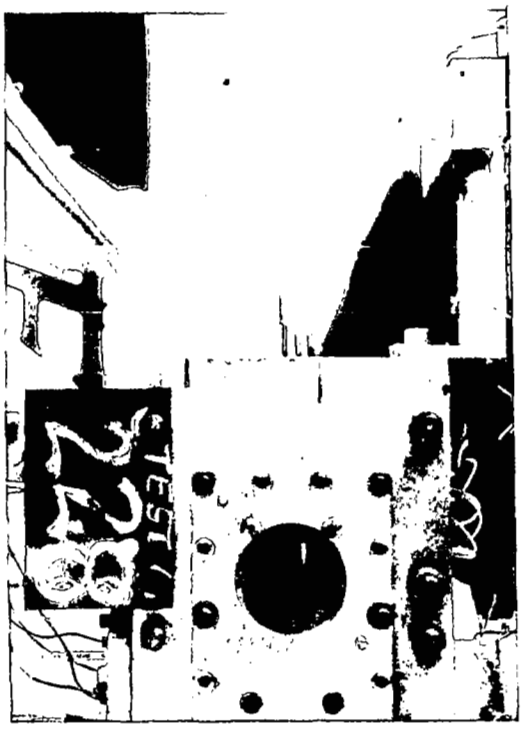

(a) Luminosity photograph taken perpendicular to the tunnel.

Figure No. 17

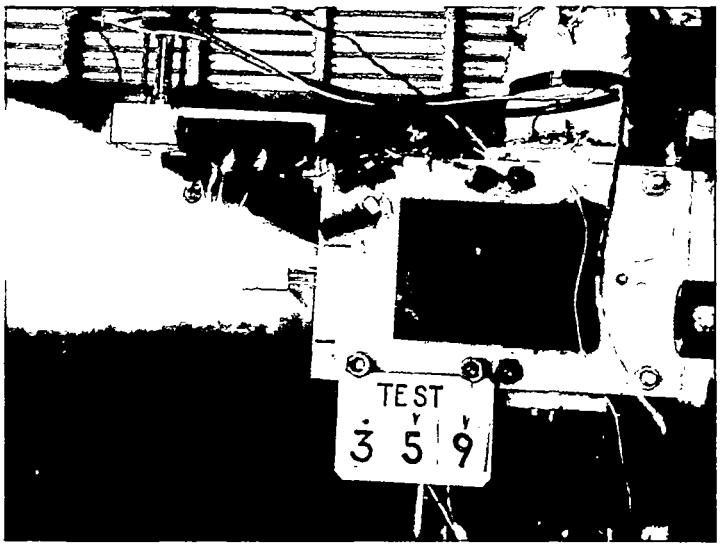

Figure No. 18 - Luminosity photograph, To,AIR = 1670°K, To,H_2 = 780°K, φ = 0.75

Figure No. 19 - Shadowgraph with the window in the upstream location, large slot with injection, φ = 1.

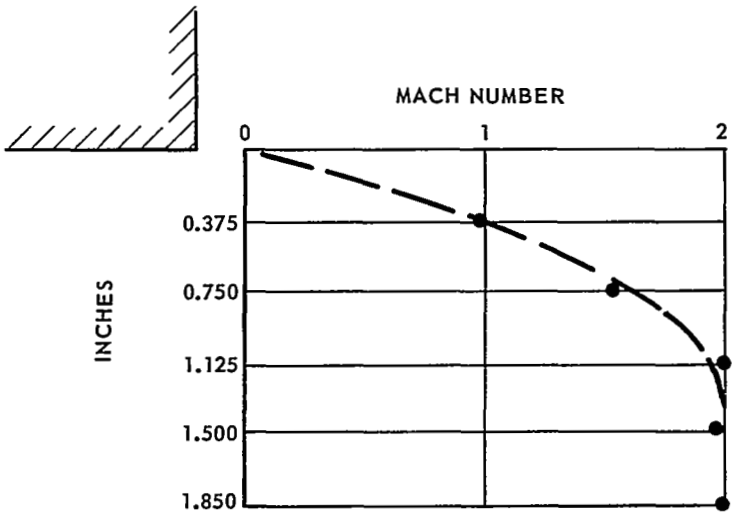

Fig. 20 MACH NUMBER DISTRIBUTION FOR To, AIR = 1670°K, To, H_2 = 780°K, φ = 0.75

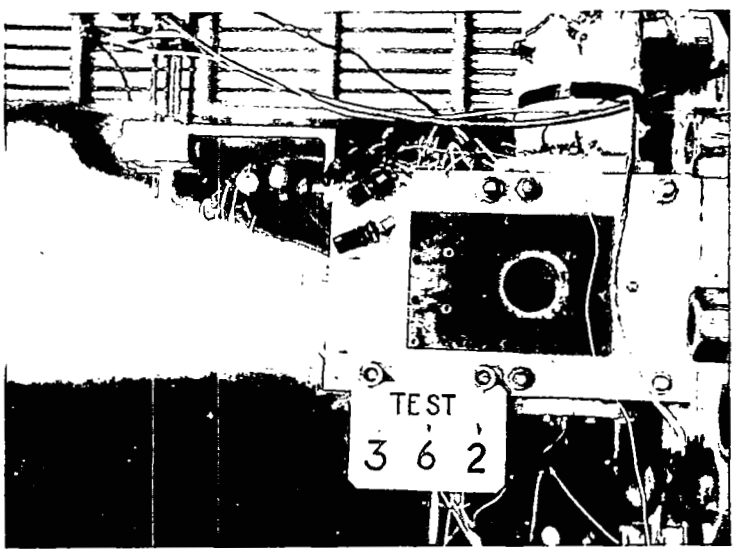

Figure No. 21 - Luminosity Photograph, To, AIR = 1500°K, To, H_2 = 780°K, φ = 0.75

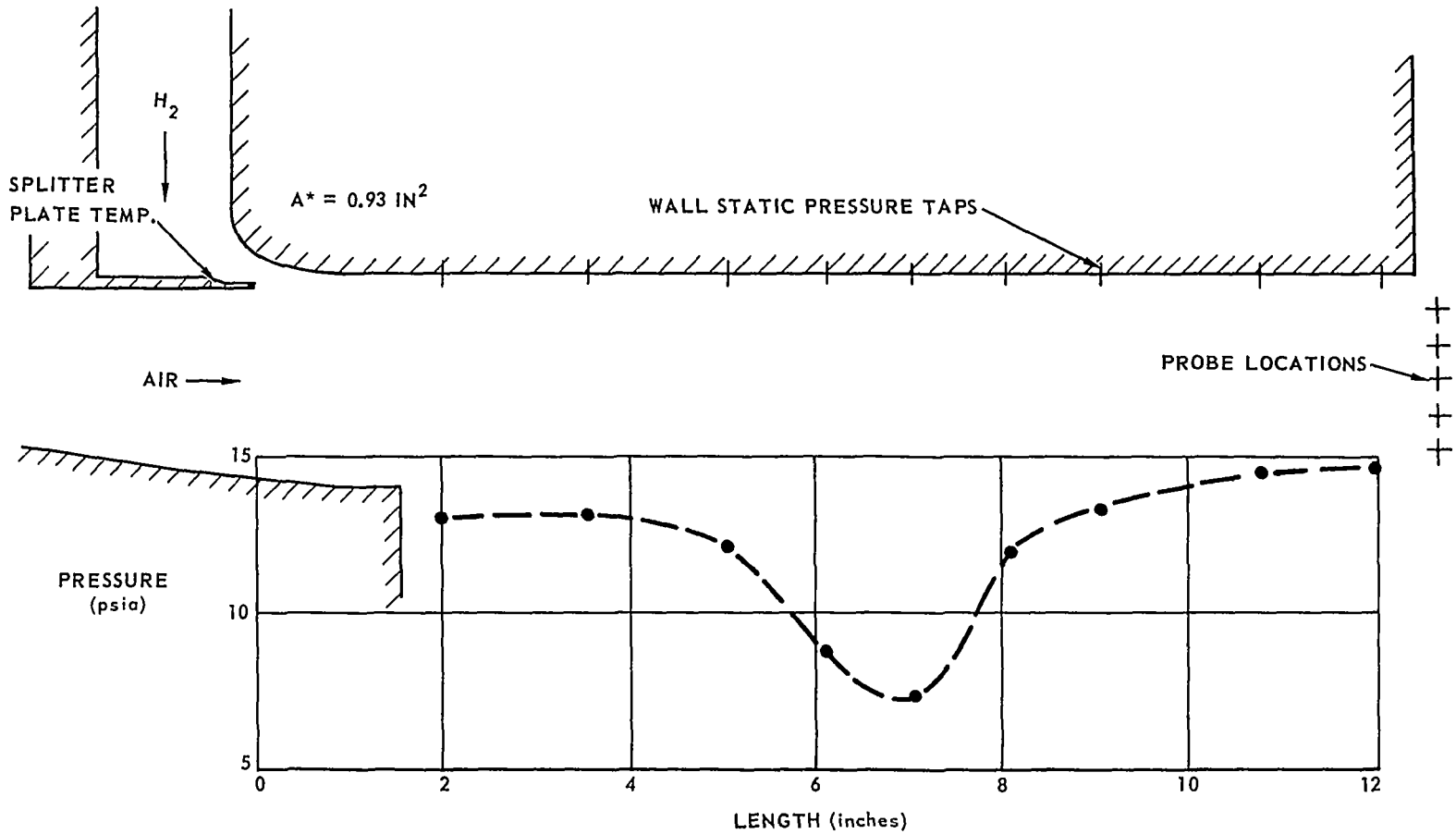

Fig. 22 STATIC PRESSURE DISTRIBUTION – To, AIR = 1500°K, To, H_2 = 780°K, φ = 0.75

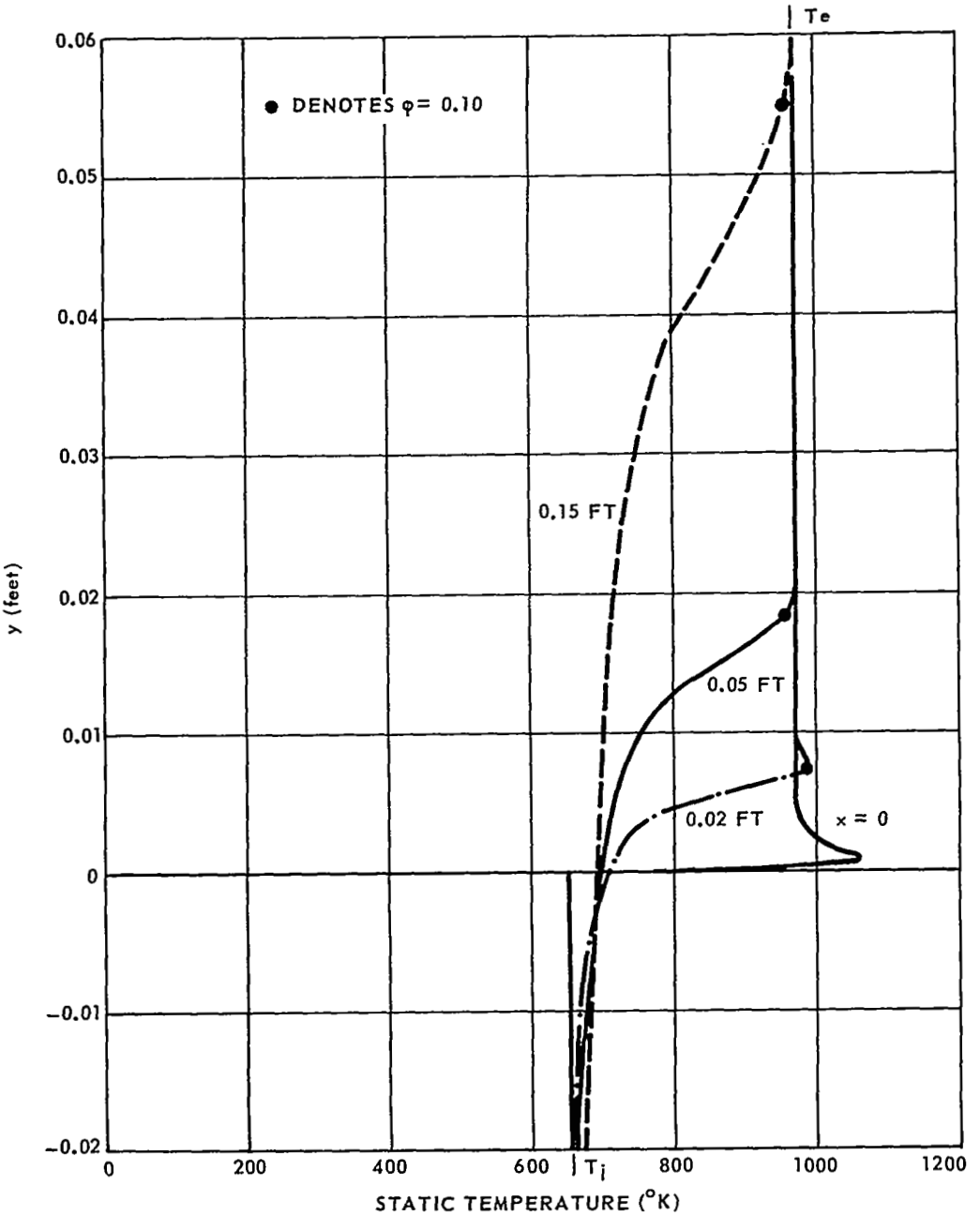

Fig. 23 TEMPERATURE PROFILES AT SEVERAL AXIAL STATIONS AS PREDICTED BY ANALYSIS FOR THE TEST CONDITIONS